PNNL-16585

Pacific Northwest
National Laboratory
Operated by Battelle for the
U.S. Department of Energy

Development of Waste Acceptance Criteria at 221-U Building: Initial Flow and Transport Scoping Calculations

V. L. Freedman
Z. F. Zhang
J. M. Keller
Y. Chen

May 2007

Prepared for the U.S. Department of Energy
under Contract DE-AC05-76RL01830

DISCLAIMER

PACIFIC NORTHWEST NATIONAL LABORATORY
operated by
BATTELLE
for the
UNITED STATES DEPARTMENT OF ENERGY
under Contract DE-AC05-76RL01830

Printed in the United States of America

Available to DOE and DOE contractors from the
Office of Scientific and Technical Information,
P.O. Box 62, Oak Ridge, TN 37831-0062;
ph: (865) 576-8401
fax: (865) 576-5728
email: reports@adonis.osti.gov

Available to the public from the National Technical Information Service,
U.S. Department of Commerce, 5285 Port Royal Rd., Springfield, VA 22161
ph: (800) 553-6847
fax: (703) 605-6900
email: orders@ntis.fedworld.gov
online ordering: http://www.ntis.gov/ordering.htm

 This document was printed on recycled paper.

PNNL-16585

Development of Waste Acceptance Criteria at 221-U Building: Initial Flow and Transport Scoping Calculations

V. L. Freedman
Z. F. Zhang
J. M. Keller
Y. Chen

May 2007

Prepared for the U.S. Department of Energy
under Contract DE-AC05-76RL01830

Pacific Northwest National Laboratory
Richland, Washington 99354

Summary

This report documents numerical flow and transport simulations that were performed under a contract from Fluor Hanford, Inc. to establish initial waste acceptance criteria for the potential waste streams that may be safely sequestered in the 221-U Building and similar canyon structures. Specifically, simulations were executed to identify the maximum loading of contaminant activity (without considering volume limitations) that can be emplaced within the 221-U Building with no more than 1 pCi/m^2 of contaminant exiting the bottom of the structure within a 1,000 year time period. Contaminants considered in the analysis were ^{3}H, ^{90}Sr, ^{99}Tc, ^{113}Cd, ^{129}I, ^{137}Cs, and ^{238}U. The initial scoping simulations were executed in one dimension to assess important processes, and then two dimensions to establish waste acceptance criteria. Two monolithic conditions were assessed: (1) a grouted canyon monolith and (2) a canyon monolith filled with sand. A three-stage approach was taken to account for different processes that may affect the amount of contaminant that can be sequestered safely in the canyon structure. In the first stage, flow and transport simulations established waste acceptance criteria based on a linear (K_d) isotherm approach. In the second stage, effects of thermal loading were examined, and the differences in waste acceptance criteria were quantified. In the third stage of modeling, precipitation/dissolution reactions were considered using reactive transport simulations, and the subsequent effect on the maximum contaminant loading was evaluated. The reactive transport modeling demonstrates a reactive transport capability that can be used for future performance predictions once site-specific data have been obtained.

Results of the simulations demonstrated that contaminants that were transported with water flow and did not undergo retardation (e.g., ^{99}Tc and ^{3}H), cannot be safely sequestered in the 221-U Building using the waste stabilization approach assumed in this study. By contrast, the amount of moderately to strongly retarded (e.g., $K_d \geq 1.0$) contaminants such as ^{238}U and ^{113}Cd that can be safely sequestered was immense, far exceeding known inventories at the Hanford Site. For contaminants that were only slightly retarded (e.g., $0 < K_d < 1.0$), specific limits on waste acceptance were established, but uncertainties in the K_d and half-life may introduce significant uncertainties in the estimated maximum loading capacities.

The simulations demonstrated that the use of grout or sand as backfill material had little effect on establishment of waste acceptance criteria. A sensitivity analysis of the preclosure barrier recharge rate demonstrated only a small effect on the flux through the contaminant source and hence a small effect on the waste acceptance criteria. This was due to a surface gravel layer that permitted runoff to flow around the concrete structure of the 221-U Building.

Heat loading had a more significant effect on the maximum loading due to increases in diffusive transport and saturated hydraulic conductivities. When the waste form was assumed to have a constant temperature of ~150ºF, maximum loading estimates decreased by 2 to 4 times the estimates when heat effects were considered to be negligible. For the more strongly retarded species, ^{238}U and ^{113}Cd, the estimates differed by several orders of magnitude. However, the maximum loading was still immense and exceeded known inventories.

When precipitation/dissolution reactions were considered, mineral volume changes generated changes in the porosity, and subsequent changes in both the diffusional release and diffusional transport rates. Although only small changes in porosity were observed (2 to 5%), the maximum loading estimates increased an average of ~5%. Although porosity increased in all of the near-field materials, it decreased

in the cementitious waste form, delaying the transport of contaminants from the source. Changes in the diffusional release rate were negligible and did not affect maximum loading estimates. Although the overall impact from precipitation/dissolution estimates was small, it is expected to be much higher once faster, temperature-dependent reaction rates are considered. Furthermore, a more mechanistic approach for describing sorption/desorption will be necessary once data on the waste formulation is available. Potential chemical interactions among the different contaminants will also need to be considered, as well as minerals that will control the release of the different contaminants. This will add scientific defensibility to future performance assessments of the 221-U Building for waste sequestration.

It is important to emphasize that the waste acceptance criteria established in this report are based on several assumptions, including the absence of cracks and fissures in the engineered materials and no volume limitations for contaminant sequestration. In addition, it was assumed that using data that is not site specific for the waste formulation and source release rates was appropriate to represent the potential waste streams at the 221-U Building. The defensibility of the waste acceptance criteria provided in this report can be determined once site-specific experimental data are acquired. While the current contaminant loading estimates satisfy the requirements for initial scoping calculations, a more defensible representation of source release rates, chemical interactions, and transport behavior is required to reduce the uncertainty in the waste acceptance criteria for future performance assessments.

Acknowledgments

The authors thank Jeff Serne, Ken Krupka and Yilin Fang of the Pacific Northwest National Laboratory (PNNL) for providing guidance and background material that directed this work. Additional thanks go to Glenn Hammond at PNNL for providing his expertise in source coding, as well as a technical review of this report.

Contents

Figures

Tables

1.0 Introduction

In 2005 the U.S. Department of Energy (DOE) and U.S. Environmental Protection Agency (EPA), with concurrence of the State of Washington, signed a Record of Decision (ROD) that set forth the final remedial action for the 221-U Building within the U Plant Area at the Hanford Site. Remedial actions identified in the final ROD include:

- Consolidation of contaminated equipment on the deck into the below-grade cells
- Backfilling (with sand or grout) of internal vessel spaces, cells, galleries, pipe trenches, drain headers, and other spaces within the building
- Removal of roof and wall sections of the 221-U Building down to approximately the deck level and their placement on or near the deck
- Construction of an engineered barrier over the remnants of the 221-U Building.

The 221-U Building is serving as a pilot for remediation of the four other canyon buildings on the Hanford Site as part of the Canyon Disposition Initiative (CDI). The CDI is a program developed to identify end states for the canyon buildings and to evaluate the potential for using the facilities for safe disposal of waste from other Hanford cleanup actions.

This report documents numerical flow and transport simulations that were performed by the Pacific Northwest National Laboratory (PNNL) under a contract from Fluor Hanford that will be used to develop waste acceptance criteria for the potential waste streams that may be safely sequestered in 221-U Building and other canyon structures. Specifically, simulations were executed to identify maximum contaminant mass and types that can be emplaced within the 221-U Building so that no more than 1 pCi/m^2 of contaminant will exit the bottom of the structure within 1,000 years. One-dimensional scoping simulations were performed to identify important processes that needed to be represented in two-dimensional simulations. The scoping simulations included reactive transport considerations to evaluate solid-aqueous phase reactions that alter the porosity of the cementitious waste and its effect on contaminant transport. In addition, one-dimensional simulations were performed to explore the sensitivity of distribution coefficients (K_d) on contaminant loading. Two-dimensional simulations were also executed to determine the maximum contaminant loading and the sensitivity of recharge. Both the one-dimensional and two-dimensional simulations considered two monolithic conditions: 1) a grouted canyon monolith and 2) a canyon monolith filled with sand.

This work is a continuation of previous modeling studies performed by Rockhold et al. (2004) and Zhang and Xie (2005). Rockhold et al. (2004) conducted contaminant transport simulations of a grouted canyon monolith using a 14-m-high by 41-m-wide simulation domain to represent a cross section of the 221-U Building and contaminant inventory provided in Jacques (2001). The primary objective of the simulations was to provide estimates of the potential migration rates of residual contaminants from the 221-U Building during the first 40 years after decommissioning. The results indicated that, under the simulated conditions, none of the modeled contaminants migrated beyond the building. Zhang and Xie (2005) extended the modeling domain used by Rockhold et al. (2004) vertically to 83 m, incorporating the groundwater table, and horizontally to 80 m. Zhang and Xie (2005) explored the effects of an engineered barrier on contaminant transport by varying the recharge rates. The simulations showed that, during the

1,000 year simulation period, all radionuclides except ^{129}I remained within the 221-U Building as long as an engineered surface barrier was emplaced. The ^{129}I, however, was simulated as a sensitivity case and is not one of the contaminants of concern at the 221-U Building.

The conceptual model, including boundary conditions and material properties used in the present work, is consistent with the conceptual models used by both Rockhold et al. (2004) and Zhang and Xie (2005). The primary difference between this study and those in the past is that past studies assumed existing contaminant distributions and the immediate availability of the contaminant for transport, whereas this study assumes contaminants are sequestered in a cementitious waste form and released at a rate dependent on properties of the contaminant and cement material.

This report is organized into four major sections. This remainder of this section describes the 221-U Building and the code used. Section 2 presents the numerical model, the simulations performed, and the parameters used. Section 3 presents the simulation results, and Section 4 contains the conclusions. Cited references are provided in Section 5. In addition, appendixes are included that provide the physical, hydraulic, chemical and transport parameters used.

1.1 Overview of the 221-U Building

One of five canyon buildings on the Hanford Site, referred as such because of their enormous size and cavernous interior, the 221-U Building lies within the U Plant Area. The U Plant Area includes ancillary structures, underground pipelines, and soil waste sites and occupies approximately 0.76 km^2 (0.3 m^2) within the 200 West Area.

The 221-U Building is a large, concrete structure approximately 800 ft long, 70 ft wide, and 80 ft high with approximately 30 ft of the height below grade. The walls and floor of the building are reinforced concrete that range from approximately 3 to 9 ft thick. A single large room extends the entire length of the building, and additional rooms called galleries are adjacent to the large room. Below the deck of the large room are the processing cells as well as a pipe trench and ventilation tunnel. A cross section of the 221-U Building is presented in Figure 1.1.

The 221-U Building was completed in 1945 as a bismuth-phosphate chemical separations plant to extract plutonium from irradiated fuel rods. Because production goals were being met by existing separation facilities, the 221-U Building was never used for its original intended purpose; instead, it was used to train the operators of other separation facilities. In 1952, the 221-U Building was converted to perform the tributyl phosphate (TBP) process to recover residual uranium from the separated wastes generated in B Plant and T Plant separation facilities. The 221-U Building served in this capacity until 1958, when it was placed in standby mode and eventually retired. All TBP process hardware was flushed and cleaned in 1957 and remains in place. Decontamination and reclamation activities occurred at the 221-U Building from 1958 to 1964, resulting in residual contamination of radionuclides and chemical contaminants. The nature and extent of this contamination has been explored by several characterization activities (DOE-RL 1998, BHI 1999, Jacques 2001). The 221-U Building is now used to store legacy equipment.

Residual contamination within the 221-U Building was not considered in this analysis. Rather, specific contaminants known to exist in Hanford Site waste, having a range of transport behaviors, were assumed to be sequestered in a cementitious waste form within a process cell of the 221-U Building.

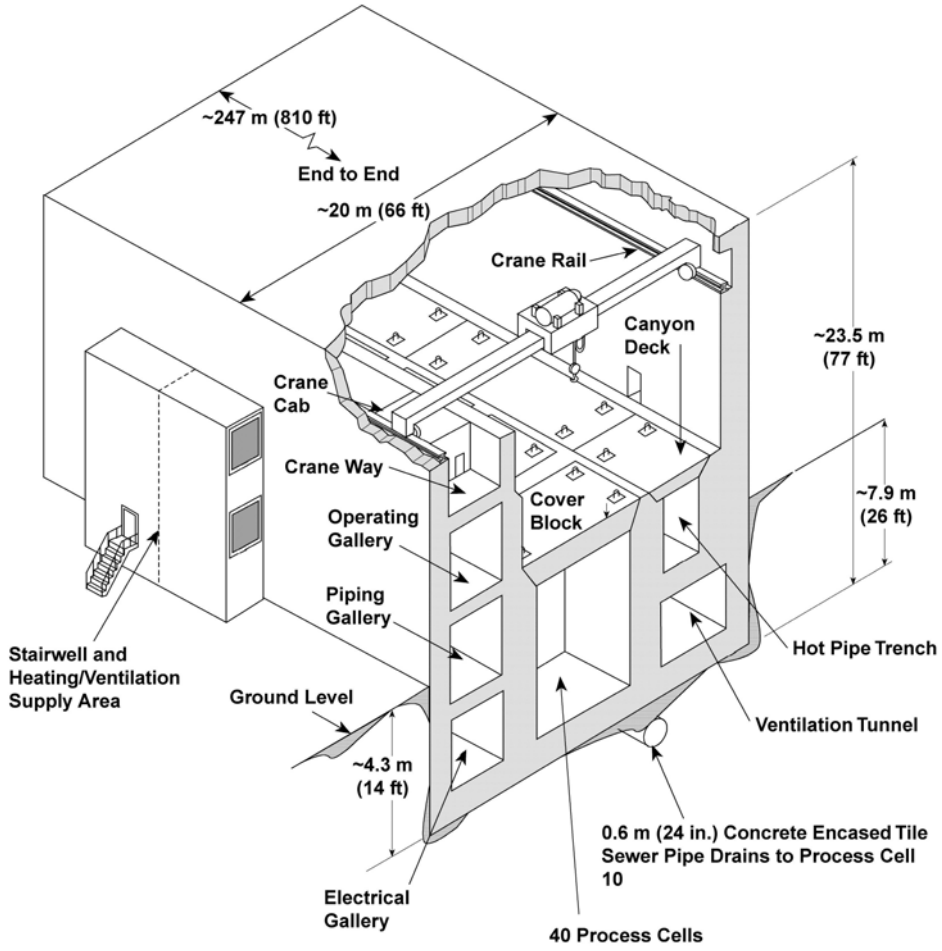

Figure 1.1. Cross Section of 221-U Building (Jacques 2001)

1.2 Code Description

Numerical simulations of contaminant transport from the 221-U Building were conducted using the STOMP simulator (White and Oostrom 2006). STOMP is a numerical model that simulates heat and mass transfer through multiple fluid phases in porous media systems. STOMP has been used to support several performance and risk assessments across the Hanford Site (e.g., Zhang et al. 2003, 2004; Freedman et al. 2005), and meets NQA-1-2000 software requirements as well as those specified under DOE Order 414.1C for Safety Software.

Three different operational modes of STOMP were used for the simulations: STOMP-W, STOMP-WAE, and STOMP-W-R. STOMP-W (Water mode) solves a single governing equation for the mass balance of liquid water under isothermal conditions and separate mass balance equations for advection and diffusion/dispersion of aqueous-phase solutes. STOMP-WAE (Water-Air-Energy mode) solves coupled equations of liquid water, air, and thermal energy; and separate mass balance equations for the advection and diffusion/dispersion of aqueous and gas phase solutes. STOMP-WAE was used to investigate heat loading and the impacts of thermal gradients on solute transport. STOMP-W-R [Water

Reactions (ECKECHEM) mode] also solves the single governing equation for the mass balance of liquid water under isothermal conditions and separate mass balance equations for advection and diffusion/ dispersion of aqueous-phase solutes. In addition, STOMP-W-R solves nonlinear equations describing mixed equilibrium and kinetic reactions. STOMP-W-R was used to investigate aqueous and solid phase reactions between the waste streams and near-field materials. Complete descriptions of the governing equations and numerical methods used in STOMP are given by White and Oostrom (2000) and White and McGrail (2005).

In the STOMP-W-R simulations, the initial conditions and boundary conditions of the system's chemical species were identified using the reactive transport simulator CRUNCH (Steefel 2001, Steefel and Yabusaki 1996). CRUNCH simulates reaction paths by solving a mixed system of equilibrium and kinetic reactions for aqueous and surface complexation, ion exchange and mineral precipitation and dissolution.

2.0 Modeling Approach

Several processes will likely affect the amount of waste (i.e., maximum contaminant loading) that can be safely sequestered in the 221-U Building. These include geochemical processes such as adsorption/desorption and precipitation/dissolution, as well as heat effects. In the initial scoping calculations presented in this report, three separate sets of simulations were used to assess these effects. In the first set of simulations, flow and solute transport simulations were carried out to determine the maximum loading when heat effects are considered to be negligible. The only chemical reaction considered was the using a distribution coefficient (K_d) that assumes linear and reversible sorption. This set of simulations was considered a base case for determining the waste acceptance criteria because it accounted for primary processes likely controlling contaminant loading in the 221-U Building. For all simulations, porous media were assumed to have no cracks or fissures that could cause preferential flow.

In the other two sets of simulations, other potential factors that could affect the maximum contaminant loading in the building were examined. For example, the second set of simulations examined the effect thermal loading had on establishing the waste acceptance criteria. In a third set of simulations, the potential effects of precipitation/dissolution reactions on establishing the waste acceptance criteria were considered. In this set of simulations thermal flow was not considered, and the effect that elevated temperatures in the building may have had on reaction rates was also ignored.

The maximum loading was determined by executing a series of forward simulations using an initial guess for the total activity of a contaminant. If the cumulative contaminant activity exceeded 1 pCi/m^2 at the bottom of the 221-U Building after 1000 years of simulation, the total contaminant activity present at the start of the simulation was reduced until the criterion was met. If the cumulative activity was less than 1 pCi/m^2, a series of forward simulations was executed until the cumulative activity at the bottom of the structure approached 1 pCi/m^2 but did not exceed this criterion.

The simulations presented in this report are considered initial scoping calculations and as such have not fully integrated all of the potential processes into a single analysis. The results demonstrate the importance of considering processes outside the basic approach shown in the base case. At this stage, no data are available to perform a more detailed analysis that fully integrates thermal and reactive transport. The approach described in this report serves as a prototype for future modeling efforts that integrate both data and modeling to add technical defensibility to future performance predictions.

2.1 Procedure

A two-step approach was used in performing the simulations. First, one-dimensional simulations were executed to scope the effects of the backfill material (sand versus grout) and dimensionality. One-dimensional simulations were also used to explore the sensitivity of distribution coefficients between 0 and 1. Second, simulations were performed to establish contaminant load limits for a two-dimensional domain. A sensitivity analysis of the prebarrier recharge rate was also performed in two dimensions.

The conceptual model and material properties were based on previous 221-U Building assessments (Rockhold et al. 2004, Zhang and Xie 2005) and the Hanford vadose zone hydrogeology data package

(Last et al. 2006). This section describes the modeling scenarios, model domain, and assigned model parameters used in this work.

2.2 Modeling Stages

At present, no published data are available for quantifying the release of contaminants of concern from waste forms that will be solidified in a cement-based waste form and stored in the 221-U Building. There is, however, a large database of contaminants that leach after being solidified in pure portland cement and mixed cement, slag, and fly ash waste forms. This diffusion release model is applied in this study to all three stages of the simulation modeling.

2.2.1 Flow and Solute Transport Simulations (STOMP-W)

Radionuclide transport in the 221-U Building is simulated using flow and transport simulations that 1) did not consider more mechanistic processes for sorption and 2) ignored the impacts of thermal loading. This set of simulations was considered the base case because, at a minimum, it considered major processes controlling the maximum loading in the 221-U Building. The linear adsorption model (i.e., K_d approach) was implemented as a useful and practical approach for modeling contaminant adsorption in transport performance assessments. The empirical approach is simple, and a considerable database of Hanford-specific K_d values is available, as are K_d values for contaminants sequestered in a cementitious waste form.

STOMP-W (Water) was used to perform the flow and solute transport simulations. Both one- and two-dimensional simulations were carried out to identify contaminant loading in the 221-U Building. Maximum loadings were determined for when grout and sand were used as a backfill material.

2.2.2 Flow Heat and Solute Transport Simulations (STOMP-WAE)

Radionuclides sequestered in the cementitious waste form have the potential to generate heat, which may affect the maximum contaminant loading in the canyon structure. At high temperatures, several non-linear phenomena must be taken into account in the simulation, such as heat conduction, vapor diffusion, and latent heat transfer due to water phase change. To date, no experimental data are available on the amount of heat that may be generated. Because concrete is expected to maintain its structural integrity up to 150ºF (65.5ºC), it was assumed that the heat generated by the cementitious waste form did not exceed this temperature.

The only contaminant expected to volatilize and be transported in the air phase was tritium. All other contaminants were assumed to be transported in the liquid phase only, and any changes in the maximum amount of contaminant that could be sequestered in the 221-U Building were due to the effects of diffusive transport.

STOMP-WAE (Water-Air-Energy) was used to perform the flow, heat, and solute transport simulations. Both one- and two-dimensional simulations were carried out to identify potential effects on contaminant loading due to heat. It was assumed that once the waste form was emplaced its temperature was 150ºF (65.5ºC). Maximum loading was determined for grout and sand as backfill material and reported as a relative loading to the base case (STOMP-W) simulations.

2.2.3 Flow and Solute and Reactive Transport Simulations (STOMP-W-R)

Radionuclide transport in the 221-U Building will be influenced by various geochemical processes that will need to be identified and described in a scientifically defensible manner. Adsorption/desorption (including ion exchange) and precipitation/dissolution are considered the most important processes affecting radionuclide interactions with sediments (Krupka and Serne 2001). Precipitation/dissolution reactions are likely to be important processes in the near-field environment where elevated concentrations of the dissolved radionuclides exist in the building.

Because no waste formulation or contaminant release data are available, data from other cement waste forms that have been reported in the literature were used. In the absence of site-specific data, more mechanistic approaches that describe contaminant releases (e.g., solubility controls) and contaminant transport (e.g., ion exchange) were not implemented in this initial scoping study. In addition, potential chemical interactions among the sequestered and residual contaminants in the 221-U Building were not considered. Rather, a framework for a reactive transport analysis was developed by examining potential impacts on contaminant loading due to changes in the porosity of the media. For future analyses, the availability of site-specific data will add technical defensibility to future performance predictions.

STOMP-W-R (Water-Reactions) was used to perform the reactive transport simulations. The chemical reactions are described by kinetic rate laws, and the aqueous components are transported by advection, diffusion, and dispersion. Ion activity coefficients were represented with the Pitzer activity model for high ionic strength solutions. As the chemical reactions proceeded, mineral volumes changed with subsequent changes in the porosity. One-dimensional simulations were carried out to identify potential impacts on contaminant loading due to alterations in the porosity of the porous media. Maximum loading was determined for when grout and sand were used as a backfill material and reported as a relative loading to the base case (STOMP-W) simulations.

2.3 Conceptual Model

The conceptual model assumed that the waste was imported into a canyon structure such as the 221-U Building. Cementitious waste was consolidated into the bottom third of the process cell and, depending on the scenario, the void spaces were filled with either grout or sand. The void spaces included the part of the process cell not filled with cementitious waste, the pipe and electrical gallery, pipe trench, and ventilation tunnel. The walls and roof of the 221-U Building were removed to the ground level and an engineered surface barrier was placed over the building, extending beyond the building footprint to a distance sufficient to make side slope effects (enhanced recharge) negligible on the underlying waste. The engineered surface barrier was not present for the first 10 years but was in place for the remaining 990 years of the simulation. The model assumed the grout and concrete did not contain cracks, joints, or fissures that would act as preferential pathways for water flow.

The STOMP-W simulations (flow and solute transport) assumed that all contaminants were transported in the liquid phase only. The STOMP-WAE simulations (flow, heat, and solute transport) assumed all contaminants except tritium were transported in the liquid phase only, with tritium also transported in the gas phase.

The two-dimensional simulation domain is described by a 41.0 x 16.9 m (134.5 x 64.3 ft) cross section of the 221-U Building and surrounding sediment. The domain extends vertically from 1 m above

the surface of the concrete structure to a depth of 15.9 m (52.2 ft) below ground surface (5.5 m, or 18.0 ft, below structure). Laterally, the domain extends 10.4 m (34.1 ft) on both sides of the concrete structure. The geological units of the simulation domain (Figure 2.2) included Hanford gravel, backfill material associated with construction of the 221-U Building (i.e., disturbed Hanford gravel), and a 0.3 m (1.0 ft) thin layer of compacted Hanford gravel, representing sediment compacted to support construction of the building. The surface of a partially demolished 221-U Building is expected to be covered with significant quantities of structural debris of varying sizes and depth. For the conceptual model in this study, a 1-m- (3.3-ft-) thick layer of gravel (0.6 m surface gravel, 0.4 m Hanford gravel) was placed above the concrete surface to represent the structural debris and to allow for unimpeded runoff from the low-permeability concrete structure.

The 221-U Building is centered in the simulation domain, with the top of the concrete structure 1 m below the top boundary of the simulation domain. The exterior dimensions of the 221-U Building are 10.4 m (34 ft) deep by 20.2 m (66.25 ft) wide. The outer cement walls of the building range from 2.6 m (8.5 ft) thick next to the pipe trench to 0.3 m (1 ft) thick above the pipe gallery. The cement thickness at the base of the building is 1.8 m (6 ft). The process cell, which contains the cementitious waste, is 6.7 m (22 ft) deep by 5.4 m (17.75 ft) wide. The bottom third of the process cell is filled with cementitious waste and the remaining top two-thirds is filled with grout or sand, depending on the simulation scenario. Figure 2.1 details the dimensions of the cement structure and void space used in the conceptual model. The cell drain and drain head below the process cell are not included in the conceptual model used for this work. Figure 2.2 presents the conceptual model of the 221-U Building and surrounding geologic units. The one-dimensional domain transected the center of the 221-U Building, incorporating the process cell.

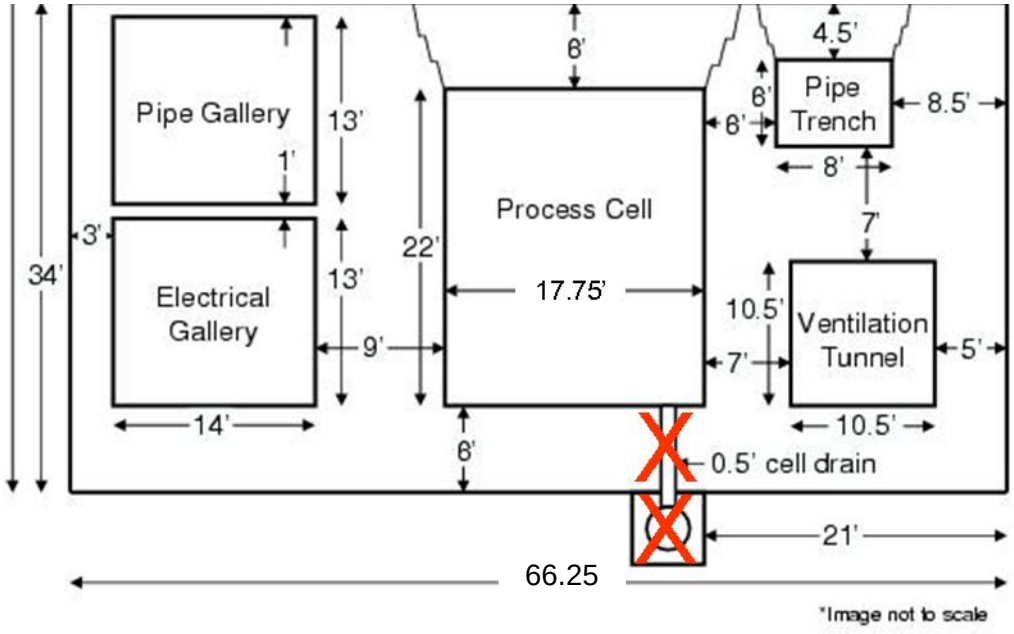

Figure 2.1. Representative Cross Section and Physical Dimensions of Below-Deck Portion of the 221-U Building. Red X designates structures not included in the conceptual model.

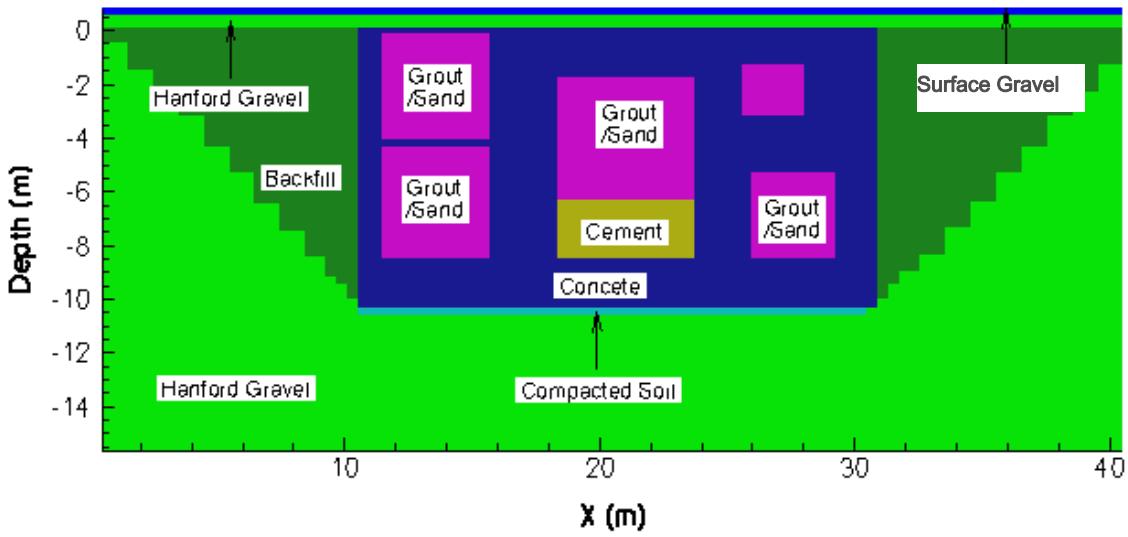

Figure 2.2. Conceptual Model of the 221-U Building and Surrounding Geologic Units

Vertical node spacing for both one- and two-dimensional simulations was variable, ranging from 0.5 m (1.6 ft) near the base of the simulation domain to 0.02 m (0.07 ft) at the location of the cementitious waste in the process cell. Because of rapid temperature changes in the STOMP-WAE simulations, the vertical node spacing through the cementitious waste was coarsened to at least 0.08 m (0.26 ft). The horizontal node spacing used for the two-dimensional STOMP-W simulations varied from 0.3048 m (1 ft) near the lateral edges of the domain to 0.01905 (0.06 ft) at the cementitious waste. The horizontal node spacing used for the two-dimensional STOMP-WAE simulation was identical to the STOMP-W simulations except through the waste form, where the maximum horizontal node spacing was 0.08 m (0.26 ft).

2.4 Initial and Boundary Conditions

Initial flow conditions for all simulations were established using steady-state conditions calculated from 1,000 year forward simulations performed using STOMP Mode 1. The simulations invoked a constant surface flux of 100 or 43.1 mm/yr, depending on the recharge scenario considered in the main model run and a unit gradient condition across the bottom boundary. The domain used for the initial conditions simulations was identical to that used for the impending contaminant and heat transport simulations minus the waste. No solute transport was considered during the initial conditions simulations.

The heat and contaminant transport simulations started with the flow conditions established during the steady flow simulations. Depending on the recharge scenario, the first 10 years of the simulation was ascribe d a surface flux of either 100 or 43.1 mm/yr, followed by a surface flux of 3.2 mm/yr for the remaining 990 years. The assigned surface flux of 3.2 mm/yr corresponds to the placement of an engineered surface barrier over the 221-U structure after the first 10 years of the simulation. The 3.2 mm/yr value is the maximum flux allowed through the surface barrier, as set forth in the 221-U Facility ROD. For the two-dimensional simulations, the surface flux of 3.2 mm/yr was ascribed only to the surface directly above the 221-U structure. On either side of the concrete structure the surface flux remained at the pre-surface-barrier rate. Table 2.1 summarizes the surface recharge rates used in the simulations. For the reactive transport simulations (STOMP-W-R), the pH of the infiltrating rainwater was ~5.6. The composition of the rainwater is found in Appendix B.

Table 2.1. Surface Recharge Rates

Surface Condition	Recharge Rate (mm/yr)
Without a cover	100/43.1
With a cover	3.2

A recharge rate through the surface cover of 3.2 mm/yr is a higher estimate and therefore more conservative than recharge estimates used in previous 221-U assessments. Rockhold et al. (2004) assigned a value of 1.0 mm/yr, while Zhang and Xie (2005) assigned a value of 0.5 mm/yr for the first 500 years and 1.0 m/yr from 500 to 1,000 years.

For all simulations, a unit gradient condition was set at the bottom boundary of the simulation domain. Advective transport of solutes and heat (outflow boundary condition) across the bottom boundary was allowed.

2.5 Hydraulic and Transport Properties

Consistent with the modeling studies of Rockhold et al. (2004) and Zhang and Xie (2005), the constitutive permeability-saturation-capillary pressure relations for the materials in this study were represented by van Genuchten (1980):

$$\theta = \theta_r + (\theta_s - \theta_r)\left[1 + (\alpha h)^n\right]^{-m} \tag{1}$$

where θ is the volumetric water content, θ_s is the saturated water content or porosity, θ_r is the residual or irreducible water content, α, n, and m are empirical fitting parameters, and h is the soil-moisture tension. Unsaturated hydraulic conductivity was described by Mualem (1976):

$$K = K_s \frac{\left\{1 - (\alpha h)^n \left[1 + (\alpha h)^n\right]^{-m}\right\}^2}{\left[1 + (\alpha h)^n\right]^{m/2}} \tag{2}$$

where K_s is the hydraulic conductivity of the porous media when saturated with water, and $m = 1\text{-}1/n$.

The physical and hydraulic property values of the sediments and engineered materials used in this study are consistent with the values assigned by Rockhold et al (2004) and Zhang and Xie (2005). Those property values were originally obtained from published characterization studies and data packages. New to this work, compared to previous studies, is the addition of cement to the 221-U Building in the form of cementitious waste. Physical and hydraulic property values for cement were acquired from Rockhold et al. (1993) and Amiri et al. (2005). Table A.1 of Appendix A lists the physical and hydraulic properties assigned to the sediments and engineered materials composing the model domain.

Effective aqueous-phase diffusion coefficients (D_e) were estimated from (Kemper and van Schaik 1966):

$$D_e(\theta) = D_{ab}\, a \exp(\mathrm{b}\theta) \tag{3}$$

where D_{ab} is the diffusion coefficient for the species in water, and a and b are empirical parameters. D_{ab} and empirical parameters a and b for the natural and engineered materials were taken from Kincaid et al. (1995). Diffusion coefficients used in this study are listed in Table A.2 of Appendix A. Half-lives for the radionuclides examined were obtained from online databases (EPA 2006, Chemistry Daily 2007) and are presented in Table 2.2 in the section that follows.

For the STOMP-WAE simulations the thermal conductivity-saturation relations for the materials in this study were represented by Cass et al. (1984):

$$\lambda = a + b\frac{\theta}{\theta_s} - (a-d)\exp\left[-\left(c\frac{\theta}{\theta_s}\right)^e\right] \tag{4}$$

where λ is the thermal conductivity, θ is the water content, θ_s is the saturated water content or porosity, and a, b, c, d, and e are empirical fitting parameters.

2.6 Selected Contaminants

The contaminants selected for analysis were chosen to provide a range of transport characteristics as they relate to reactivity with the natural and engineered materials. The radionuclides modeled and their reactivity characteristics are presented in Table 2.2. Technetium (^{99}Tc) and tritium (^{3}H) represent conservative species with respect to transport, with ^{3}H also representing a decay species (relatively short half-life). In addition, ^{3}H is unique from other contaminants considered in that it has the propensity to exist in significant quantities in the gas phase. Uranium (^{238}U) represents a highly reactive species that does not undergo significant decay. Strontium (^{90}Sr) and cesium (^{137}Cs) both represent moderately reactive contaminants and decay species. Iodine (^{129}I) and cadmium (^{113}Cd) were also included in the analysis given the likelihood of their presence in the sequestered waste form.

Table 2.2. Contaminants Selected for Analysis and Their Reactivity Characteristics

Radionuclide	Rationale for Selection	Half-Life (yr)[(a)]
^{99}Tc	Conservative	2.13×10^{5}
^{3}H	Conservative w/ decay	12.3
^{238}U	Highly reactive	4.46×10^{9}
^{90}Sr	Moderately reactive w/ decay	29.1
^{137}Cs	Moderately reactive w/ decay	30.0
^{129}I	Moderately reactive	1.57×10^{7}
^{113}Cd	Highly reactive	7.7×10^{15}
(a) The half-life of ^{113}Cd from Chemistry Daily (2007); half-life for all other radionuclides from EPA (2006)		

2.7 Distribution Coefficients (K_d)

Radionuclide sorption on sediments can be quantified by the use of a partition (or distribution) coefficient, K_d. The K_d parameter is defined as the ratio of the amount of adsorbate adsorbed per mass of solid to the amount of adsorbate remaining in solution at equilibrium. The K_d is an empirical unit of measurement that accounts for several different chemical and physical retardation mechanisms. For example, when a radionuclide is in an immobile phase, it is often not known whether it is adsorbed onto the surface of the solid, absorbed into its structure, precipitated as a three-dimensional molecular structure on the surface of the solid, or partitioned into the organic matter (Sposito 1989). The term "sorption" is used to encompass all of these processes. Radionuclides that adsorb strongly have large K_d values (e.g., > 100 mL/g), whereas those that migrate at the same rate as water flow have K_d values of 0 mL/g.

In this investigation, the linear distribution coefficient was used to describe sorption. Although the reactive transport simulations using STOMP-W-R are capable of describing sorption processes more mechanistically via ion exchange or surface complexation models, the parameters needed to implement these models in the reactive transport simulator do not exist for the cement formulation assumed in this investigation. Furthermore, the contaminants of interest are not likely to be retarded due to precipitation, but rather due to sorption.

The contaminants of interest and their selected K_d values for cement are given in Table 2.3. Given the similarity in geological materials, the distribution coefficients were assumed to be the same for the cement, concrete, and grout materials. These values were obtained from Krupka and Serne (2001), which compiled K_d values from Krupka and Serne (1998) and Bradbury and Van Loon (1998). The K_d values in Table 2.3 are considered minimum values, so that radionuclide transport calculations would overpredict contaminant transport. As minimum values, the tabulated K_d values will underpredict the extent of adsorption and overpredict radionuclide transport. Following the convention of Bradbury and Sarott (1995), only the first temporal environment (the first 100 to 10, 0000 years) was considered in identifying distribution coefficients. In this environment, the cement has hardened and been wetted by infiltrating water. The cement pore water is characterized as having a high pH (~13), high ionic strength, and high concentrations of potassium and sodium resulting from the dissolution of alkali impurities in the clinker phases.

Also shown in Table 2.3 are the K_d values for the contaminants of interest associated with soil materials. These values are consistent with those used in previous 221-U Building assessments (Rockhold et al. 2004, Zhang and Xie 2005).

2.8 Initial Contaminant Distribution and Release

Previous 221-U Building simulation studies (Rockhold et al. 2004, Zhang and Xie 2005) assumed initial contaminant distributions derived from existing conditions described in the final 221-U Building characterization report (Jacques 2001). In these studies, the contaminant was assumed to be available for transport immediately. This present work differs in that contaminants are assumed to be introduced into the 221-U Building and sequestered in a cementitious waste form. Under this condition, the contaminants are assumed to be released gradually from the stabilized waste form, where they are then available for transport.

Table 2.3. Distribution Coefficients for the Geological Units

Geological Units	Radionuclide	K_d (mL/g)
Soil Sediments	Tc-99	0
	H-3	0
	U-238	1000
	Sr-90	3
	Cs-137	3
Gravel	Tc-99	0
	H-3	0
	U-238	1000
	Sr-90	2
	Cs-137	1
Concrete	Tc-99	0
	H-3	0
	U-238	1000
	Sr-90	2
	Cs-137	1
Grout	Tc-99	0
	H-3	0
	U-238	1000
	Sr-90	2
	Cs-137	1
Cement	Tc-99	0
	H-3	0
	U-238	1000
	Sr-90	2
	Cs-137	1

2.9 Contaminant Distribution and Release

Previous 221-U Building simulation studies (Rockhold et al 2004, Zhang and Xie 2005) assumed initial contaminant distributions derived from existing conditions described in the final 221-U Building characterization report (Jacques 2001). In these studies, the contaminant was assumed immediately available for transport. This present work differs in that contaminants are assumed to be introduced into the 221-U Building and sequestered in a cementitious waste form. Under this condition, the contaminants are assumed to be gradually released from the stabilized waste form, where they are then available for transport.

Release of contaminants from the cementitious form was described using a diffusion release model implemented in the STOMP simulator (Zhang et al. 2004, Freedman et al. 2005). Because little or no advection occurs through the cement material, it is appropriate to model the release of contaminants as a diffusion-limited process given as (Khaleel and Connelly 2003):

$$Q(t) = \frac{I}{d}\sqrt{\frac{D_a}{\pi t}} \tag{5}$$

where d is the source thickness, t is time, and I is the total inventory of the contaminant, defined as

$$I = C_0 \sum_i V_i = C_0 V_T \tag{6}$$

where C_0 is the initial contaminant concentration and V_T is the total volume of all release simulation cells. As part of the diffusion release model, the STOMP simulator requires user defined values of D_a and d. The source thickness was assumed to be 2.235 m, equivalent to one-third the height of the process cell. The process for obtaining diffusion release estimates (D_a) is outlined in the following section.

2.10 Diffusion Coefficients

Empirical effective diffusion coefficients measured in short-term laboratory experiments are widely used to model the long-term performance of cementitious waste forms (e.g., Atkinson and Nickerson 1988, Albenesius 2001). These measurements have changed little since the International Atomic Energy Agency (IAEA) method was proposed by Hespe in 1971 and assume linear sorption independent of concentration as well as fast and reversible kinetics. The intrinsic diffusion coefficient is a measure of the physical contribution to diffusion and depends on the tortuosity (τ), constrictivity (δ), and porosity (ε) of the cement, which influence the diffusion coefficient of the free ion in water, D_f, by the following equation:

$$D_i = D_f \frac{\varepsilon \delta}{\tau^2} \tag{7}$$

Assuming fast kinetics and a linear isotherm yields the following equation, where the modified diffusion coefficient is the apparent diffusion coefficient, D_a, and is related to the intrinsic diffusion coefficient modified by a chemical capacity factor, α.:

$$D_a = D_f \frac{\varepsilon \delta}{\tau^2 \alpha} = \frac{D_i}{\alpha} \tag{8}$$

The capacity factor is the ratio of the moles of contaminant per unit volume of water-saturated solid to the moles per unit volume of contaminant in the liquid. The capacity factor is related to the distribution coefficient, K_d (mL/g), by the following equation, where ε is porosity and ρ is the bulk density of the porous media:

$$\alpha = \varepsilon + \rho K_d \tag{9}$$

This construct is applied to the diffusion release model for quantifying the release of contaminants from the cementitious waste form. For the STOMP-W and STOMP-WAE simulations, the diffusion release rate is constant, though it will differ depending on the distribution coefficient. For the reactive transport simulations, contaminant release rates changed with time in response to alterations in the

porosity of the cement material due to solid-aqueous phase reactions. At each simulation time step, the diffusional source release rate was adjusted through a feedback loop in the diffusion release model (Eq. 8). Initial values for the diffusion coefficient are given in Table 2.4. They remain constant in the STOMP-W and STOMP-WAE simulations.

Table 2.4. Diffusion Coefficients for a Diffusion-Limited Contaminant Source

Radionuclide	Diffusion Coefficient [cm^2/s]
Tc-99	5.21E-07
H-3	5.21E-07
U-238	4.58E-11
Sr-90	4.21E-08
Cs-137	2.20E-08
I-129	4.54E-9
Cd-113	1.15E-11

2.11 Mineralogical Composition

When cementitious materials come in contact with subsurface water, a hyperalkaline pore fluid is produced with a pH in the range of 10–13.5 (Atkinson 1985, Berner 1992). Not only does the pH affect radionuclide adsorption and solubility, but the pore fluids have the potential to chemically react with near-field materials and affect physical and chemical properties. Potential reactions include a loss of swelling capacity and changes in porosity, mineralogical composition, or sorption capacity (Savage et al. 2002).

In the reactive transport simulations, impacts to changes in porosity were investigated via changes in the mineralogical composition of the cement and near-field materials. It was assumed, however, that the sorption capacity remained constant for all materials.

2.11.1 Cementitious Waste Form

Radionuclide transport through the 221-U Building will depend on several factors, including source concentration and release rate, surface recharge, heat generation, and waste package durability. In addition, several geochemical processes will influence contaminant movement, such as oxidation/reduction, aqueous speciation, adsorption/Desorption, and precipitation/dissolution. Hence, the materials selected for sequestering wastes is an important issue because the protection of waste packages from corrosion and chemical degradation can be improved by proper choices.

Portland cement has been studied extensively for the solidification and immobilization of low- and medium-level radioactive wastes (Goni et al. 2006). The primary mechanism for solidification is based on the precipitation of hydroxides from the highly alkaline pore solution of hydrated portland cement. The main products of hydration are calcium silicate hydrates (C-S-H), calcium hydroxide, calcium aluminate, and calcium ferrite. Typically, calcium silicate hydrates resemble crystalline minerals such as tobermorite and jennite (Galindez et al. 2006). Berner (1992) describes the composition of hydrated cement as

- 40–50 wt% calcium silicate hydrogel (CSH)
- 20–25 wt% portlandite [$Ca(OH)_2$]

- 10–20 wt% ettringite [$Ca_6Al_2O_6(SO_4)_3$], monosulfate [$Ca_4Al_2O_6SO_4$], and ferric phases
- 10–20 wt% pore solution
- 0–5 wt% minor components such as NaOH, KOH, and $Mg(OH)_2$.

Cesium retention, however, is low in traditional portland cement matrices. Hence, other components are introduced into the cement matrix that have a capacity for ionic exchange, such as fly ash, slags and zeolites (Goni et al. 2006).

In this study, a cement waste formulation was assumed based on the CEM-V cement, a blended portland, fly ash, blast furnace slag cement, described in Trotignon et al. (2006). The mineralogical composition and volume fractions of the CEM-V cement paste is given in Appendix B, Table B.1. Because pertinent physical properties of CEM-V were not given in Trotignon et al. (2006), properties of the cementitious waste (shown in Table A.1) were based on median values of cement physical properties measured in Amiri et al. (2005).

2.11.2 Near-Field Materials

All open galleries are assumed to be backfilled with grout or sand. The grout composition was based on Savage et al. (2002), which examined interactions of bentonite with hyperalkaline fluids. The mineralogical composition of the grout reflected the likely composition of a grout barrier that may be used in a geological disposal building (see Appendix B, Table B.2). For the sand, a low-reactivity mineral composition was assumed that was composed almost entirely of quartz (Appendix B, Table B.3).

The mineralogical composition of the concrete structure was assumed to be similar to that of the cement waste form. Unlike the cement waste form, the concrete was assumed to have a large quartz volume fraction that was added to cement for strength (Appendix B, Table B.4). The mineral volume fractions were based on data found at http://www.ce.berkeley.edu/~paulmont/CE60New/cement.pdf). All soils and gravels were assumed to have the same mineralogical composition (Appendix B, Table B.5) based on the mineralogical composition of soils assumed in the Integrated Disposal Building Performance Assessment (Bacon and McGrail 2005).

2.11.3 Secondary Mineral Precipitates

In addition to the primary minerals, the model also includes secondary minerals that may precipitate as the primary minerals undergo dissolution. These minerals were identified as possible precipitates using CRUNCH reactive transport simulator (Steefel and Yabusaki 1996, Steefel 2001), as well as minerals that had already been identified in the literature (Savage et al. 2002, Trotignon et al. 2006). Minerals were selected as being representative of the mineral types likely to form in such systems, such as zeolites, Ca silicate hydrates, and sheet silicates to represent a range of plausible products, and are shown in Appendix B, Table B.6.

Although potential secondary minerals were identified in separate simulations that only considered a single material, all minerals (both primary and secondary) were allowed to form in all of the geologic materials. Hence, the dissolution of a primary mineral could result in its precipitation downstream from its original location.

2.12 pH Behavior of the Waste Form

Of significant importance to the long-term prediction of fate and transport of contaminants is the long-term chemical reactions pathways that occur as cementitious waste forms interact with infiltrating water (Krupka and Serne 2001). Most contaminants are metal-like and sensitive to pH. When a cementitious waste form first comes in contact with water, the alkali hydroxide phases, present in relatively minor amounts, result in a high ionic strength solution with a high pH value of ~13. As these phases are leached from the cement, the pore fluid pH is buffered near 12.5 by the dissolution of free portlandite in the cement. Eventually the portlandite is depleted, and the pore fluid pH decreases to approximately 10.5, where it is controlled by the incongruent dissolution of calcium silicate hydrogel (CSH). The solubility properties of CSH, however, vary as a function of its calcium/silica ratio. Once the dissolution of CSH is complete, the pH of the cement pore fluid will continue to decrease to a value buffered by the infiltrating water. Schematically, this change of pH is shown as a function of time in Figure 2.3.

The time frame over which the pH of the pore solution changes from 13.5 to that of the ambient water is determined by the rate at which water migrates through the cement system (Krupka and Serne 2001). For example, calculations by Atkinson et al. (1989) indicate that the pH of the near-field pore water would remain above 10.5 for several hundred thousand years in radioactive waste disposal systems being considered in the United Kingdom. For a land burial ground at Hanford, Criscenti et al. (1996) showed that the pH did not go below 10 for 10,000 years because CSH gel remained to buffer the pH. In the 221-U building, the pH is expected to remain high for thousands of years, given the limited recharge that will likely move through the canyon structure.

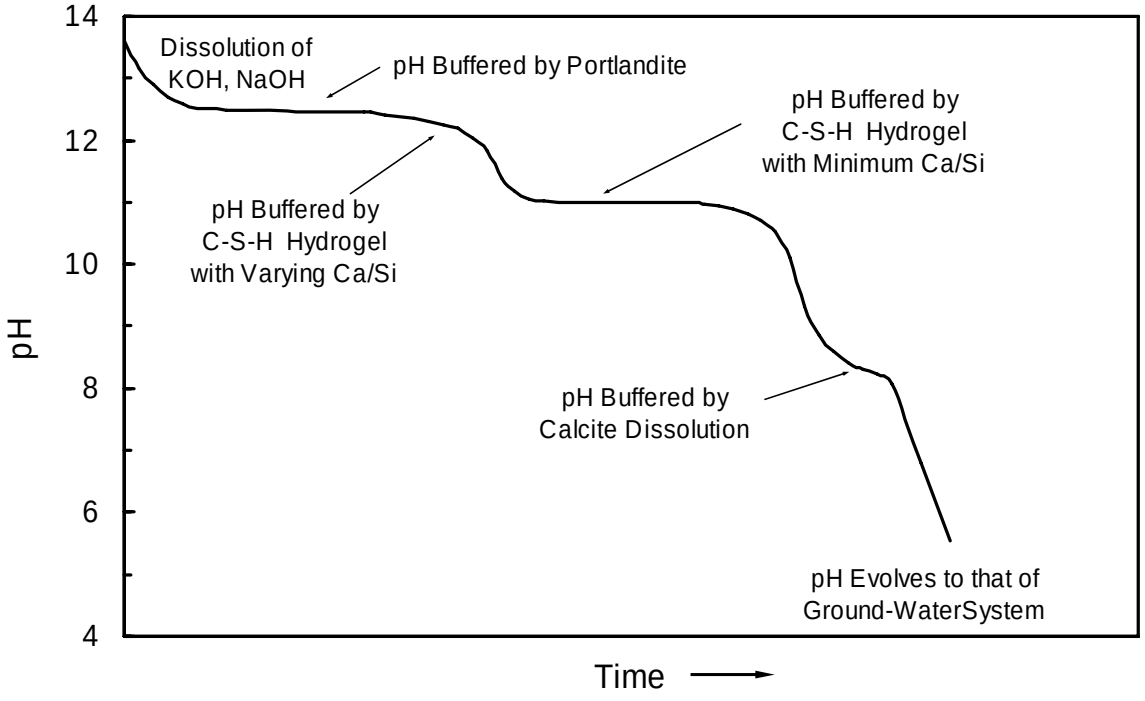

Figure 2.3. Change of Pore Water pH Resulting from Reactions of Cement Components (from Krupka and Serne 2001)

3.0 Results

Simulation results and estimated waste acceptance criteria are presented in the following sections. Three sets of simulations are presented and are distinguished by the modeling stage: flow and solute transport (STOMP-W); flow, heat, and solute transport (STOMP-WAE); flow and solute and reactive transport (STOMP-W-R). Each modeling stage evaluates maximum contaminant activity and types of contaminants that can be emplaced within the 221-U Building with no more than 1 pCi/m^2 of contaminant migrating outside the structure within a 1,000 year time period.

STOMP-W simulations assessed the maximum loading when heat impacts are considered to be negligible and the only chemical reaction considered is the use of a distribution coefficient (K_d) that assumes linear and reversible sorption. One- and two-dimensional simulations were executed, each evaluating scenarios with grout and sand backfilling the open galleries. Sensitivity cases using STOMP-W were also performed to investigate changes in acceptance criteria in response to changes in K_d, half-life, and recharge parameters. In total, six cases were evaluated using STOMP-W.

STOMP-WAE simulations examined the impact of thermal loading on establishing the waste acceptance criteria. One-dimensional simulations were used to scope the difference in maximum loading for both a grout- and sand-filled monolith. Only a grout-filled monolith was simulated in two dimensions since one-dimensional results demonstrated no significant differences in establishing the waste acceptance criteria.

STOMP-W-R simulations considered the potential effect of precipitation/dissolution reactions on establishing the waste acceptance criteria. Due to computational time constraints, simulations were limited to one dimension. The simulations assessed two cases, a grout backfill scenario and a sand backfill scenario.

3.1 Flow and Solute Transport (STOMP-W) Results

The STOMP-W simulations considered the six cases described in Table 3.1. Cases 1, 2, 3, and 4 were used to establish waste acceptance criteria in one and two dimensions and for both grout- and sand-filled monoliths. Cases 1b and 3b are considered sensitivity cases that evaluated the influence of recharge, K_d, and half-life parameters on the maximum loading estimates.

The calculated waste acceptance criteria for the one- and two-dimensional cases with grout and sand backfill are presented in Table 3.2 and Figure 3.1. The maximum loading was determined when the amount of contaminant exiting the 221-U Building exceeded 1 pCi/m2 over the 1,000 year simulation period. What was not considered in this evaluation was the physical capacity of the bottom third of the process cell where the cementitious waste is placed; i.e. the calculated maximum loading criteria may exceed the volume of the process cell available for waste disposal. The analysis also assumed that no other contaminants were present.

The maximum loading for the conservative species ^{99}Tc and ^{3}H is extremely small, less than 10^{-4} Ci/m^3. The low waste acceptance criteria for ^{99}Tc and ^{3}H suggest that these radionuclides cannot be safely sequestered in the 221-U structure. The maximum loading capacity for moderately reactive species

Table 3.1. STOMP-W Simulation Scenarios

Case	Scenario
1	**1-D** Simulation; top 2/3 of the process cell was filled with **grout**; bottom 1/3 of the process cell contained the cementitious waste form; natural recharge = 43.1 mm/yr
1b	Same as Case 1 except 0 ml/g ≤ Kd ≤ 1 ml/g and 30 yr ≤ half-life ≤ 1E20 yr
2	**1-D** Simulation; top 2/3 of the process cell was filled with **sand**; bottom 1/3 of the process cell contained the cementitious waste form; natural recharge = 43.1 mm/yr
3	**2-D** Simulation; top 2/3 of the process cell was filled with **grout**; bottom 1/3 of the process cell contained the cementitious waste form; natural recharge = 43.1 mm/yr
3b	Same as Case 3 except that natural recharge = 100 mm/yr
4	**2-D** Simulation; top 2/3 of the process cell was filled with **sand**; bottom 1/3 of the process cell contained the cementitious waste form; natural recharge = 43.1 mm/yr

Table 3.2. STOMP-W Calculated Waste Acceptance Criteria

Simulation Case	Waste Acceptance Criteria (Ci/m^3)						
	^{99}Tc	^{3}H	^{238}U	^{90}Sr	^{137}Cs	^{129}I	^{113}Cd
Case 1: 1D Grout	1.97E-09	8.97E-06	1.41E+43	6.44E+04	7.52E+07	6.84E+09	4.52E+53
Case 2: 1D Sand	1.97E-09	8.78E-06	1.39E+43	6.40E+04	7.48E+07	6.81E+09	4.47E+53
Case 3: 2D Grout	6.29E-09	3.93E-05	4.58E+43	1.05E+05	3.47E+08	1.07E+10	1.52E+54
Case 4: 2D Sand	5.30E-09	3.30E-05	4.05E+43	9.98E+04	3.33E+08	1.05E+10	1.34e+54

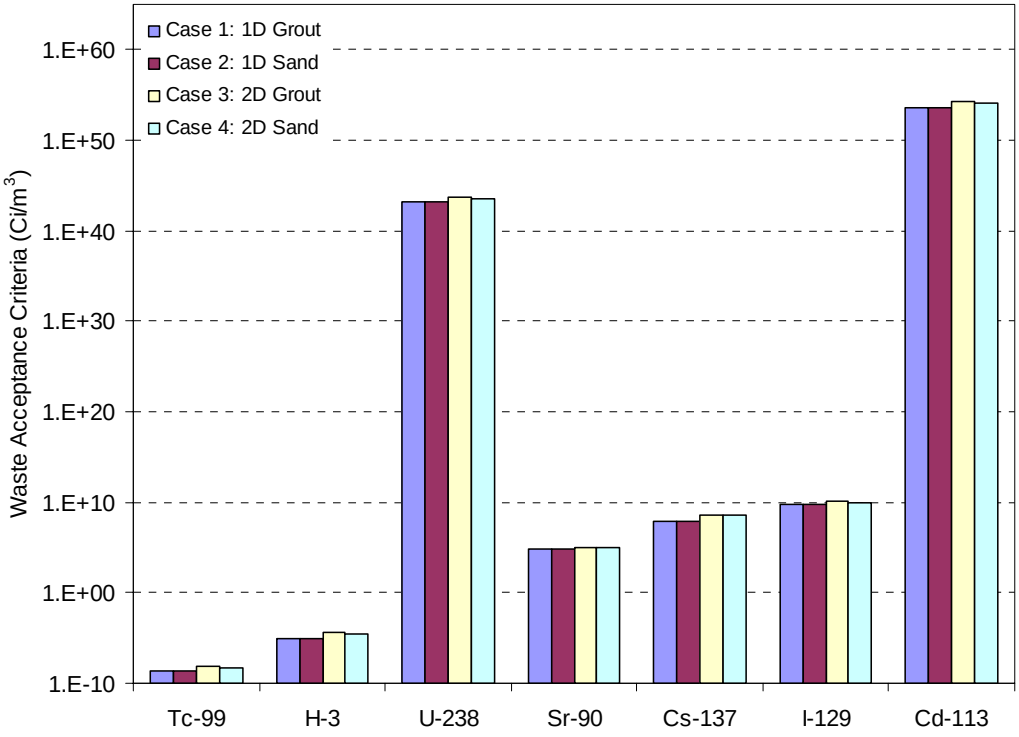

Figure 3.1. STOMP-W Waste Acceptance Criteria

was greater than 10^4 Ci/m^3 for ^{90}Sr (K_d in cement of 1 mL/g) to greater than 10^7 for ^{137}Cs and ^{129}I (K_d in cement of 2 and 10 mL/g, respectively). Loading of the highly reactive species ^{238}U and ^{113}Cd (K_d in cement of 1000 and 4000 mL/g, respectively) exceeded 10^{43} Ci/m^3 and known inventories at Hanford.

For all radionuclides the maximum loading was slightly higher when grout was used as the process cell backfill material rather than sand. In addition, calculated loading from two-dimensional simulations was higher than that calculated from one-dimensional simulations (see Section 3.1.1).

The mass (activity) fractions of the contaminants are presented in Figures 3.2 and 3.3 at 1000 years for both one- and two-dimensional simulations. Both figures demonstrate that the majority of the

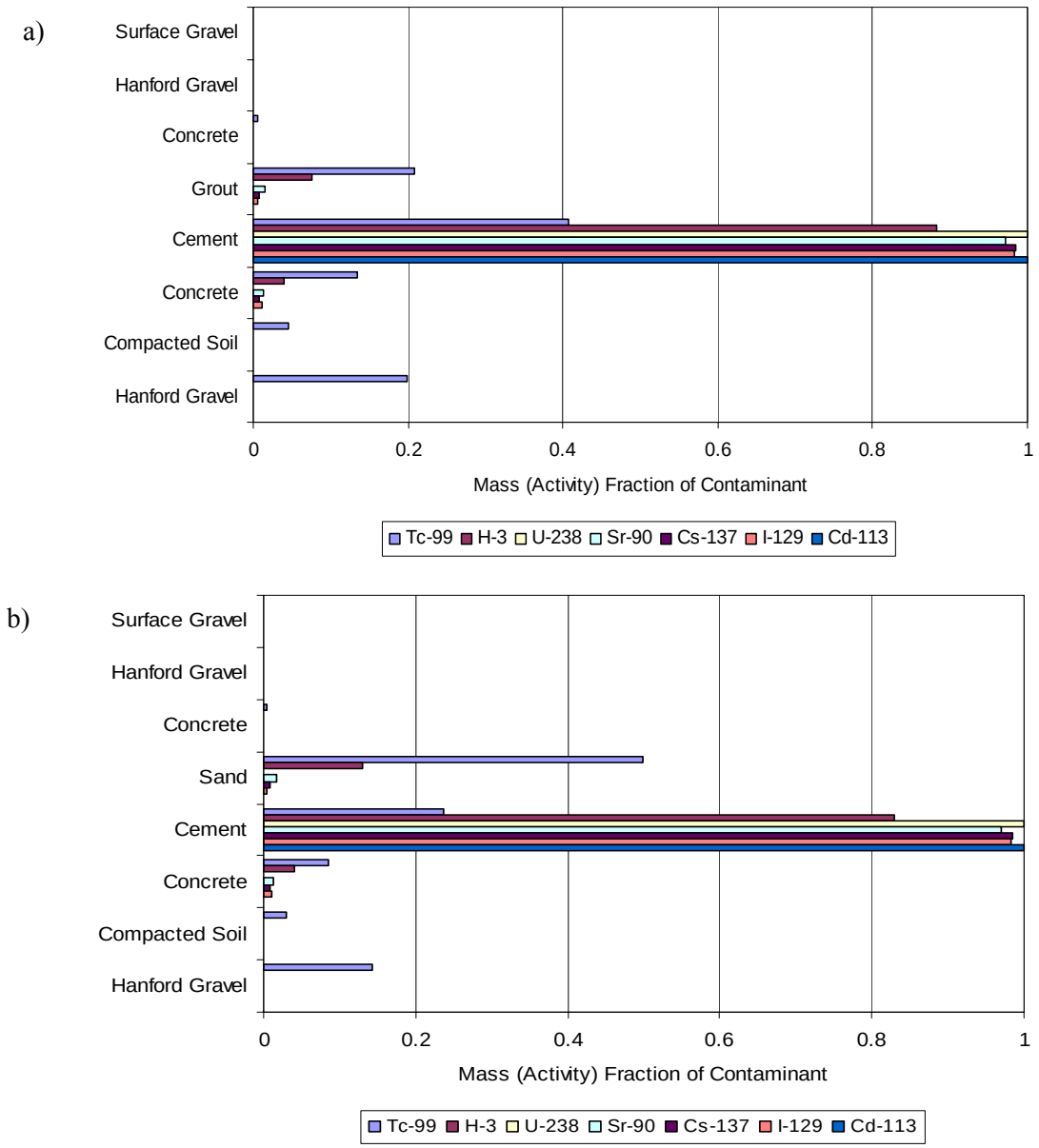

Figure 3.2. Mass Fraction of Contaminants for 1-D Model after 1000 Years of Simulation for Flow and Solute Transport (STOMP-W) for a) Grouted and b) Sand-Filled Monoliths

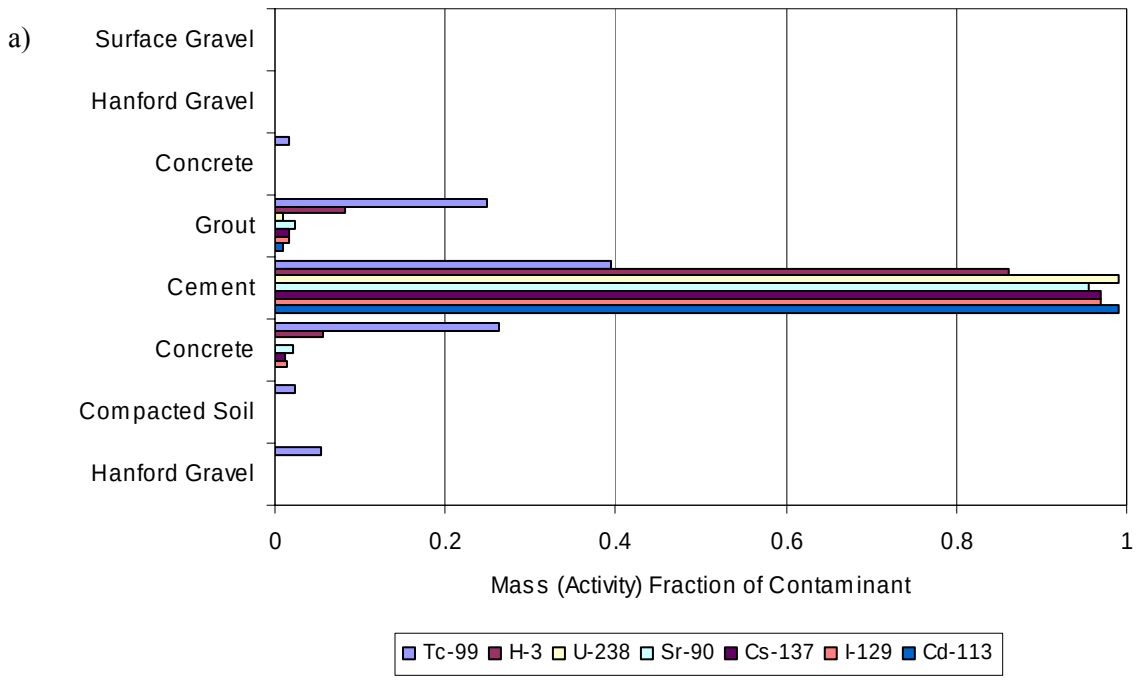

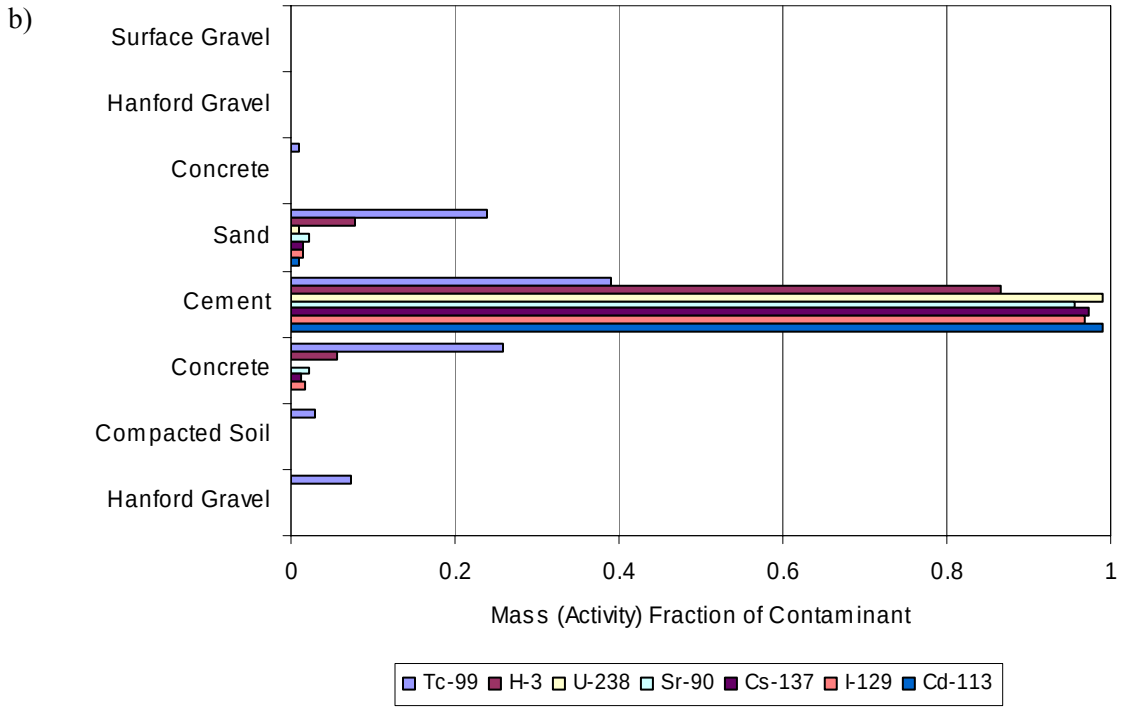

Figure 3.3. Mass Fraction of Contaminants for 2-D Model After 1000 Years of Simulation for Flow and Solute Transport (STOMP-W) for a) Grouted and b) Sand-Filled Monoliths

contaminants are still within the cementitious waste source after 1000 years of simulation. The most mobile contaminants, ^{99}Tc and ^{3}H, are present in the layers adjacent to and downstream of the cementitious waste source, whereas the less conservative contaminants, ^{113}Cd and ^{238}U, are nearly completely confined to the source area. The total concentrations of all other contaminants are also confined to the source but are present in smaller amounts in the adjacent subsurface materials and downstream. The figures also demonstrate a wider distribution of the contaminants in two dimensions, which is similar for the grout- and sand-filled scenarios. No contaminants were present in the backfill material that surrounded the 221-U Building in the two-dimensional simulations.

3.1.1 Dimensionality and Backfill Material Evaluation

A comparison of one-dimensional versus two-dimensional simulation results (Table 3.3) demonstrates that the maximum loading capacity is calculated to be larger in the two-dimensional simulations than in the one-dimensional simulations. The absence of contaminant spreading in the second dimension contributes to reduced maximum loading capacities in the one-dimensional simulations. For grout, the two-dimensional loading was on average approximately 3.1 times the one-dimensional maximum loading capacity. The maximum loading capacity for sand was on average approximately 2.8 times larger than the one-dimensional loading capacity.

Table 3.3. Relative Waste Acceptance Criteria (2D Loading Capacity/1D Loading Capacity) for Grout- and Sand-Filled Monolithss

Fill Material	Relative Waste Acceptance Criteria						
	^{99}Tc	^{3}H	^{238}U	^{90}Sr	^{137}Cs	^{129}I	^{113}Cd
Grout	3.196	4.383	3.250	1.636	4.618	1.564	3.368
Sand	2.694	3.759	2.905	1.560	4.453	1.543	2.995

A comparison of one-dimensional calculated loading capacities for grout and those calculated for sand (Table 3.4) shows no significant difference between the values. By contrast, two-dimensional maximum loading capacities were on average 1.1 times greater for grout than for sand. Although this demonstrates that grout is a better material for retaining contaminants within the process cell, the impact is not significant in terms of establishing waste acceptance criteria. For example, the maximum differences in contaminant loading resulted for both the highly mobile and the strongly retarded species. The impact is negligible for the conservative species (^{3}H and ^{99}Tc) because the amount of waste that could be safely sequestered is so small that a safer decision is to not emplace it at all within the building. For the more strongly retarded species, the maximum loadings determined in this analysis for both grout and sand were so large that they likely exceeded total inventories at the Hanford Site. Although contaminant densities were not considered, it is also likely that the loading estimates for strongly retarded species exceeded the available waste disposal volume in the 221-U Building.

Table 3.4. Waste Acceptance Criteria for Sand-Filled Monoliths Relative to Grout-Filled Monoliths

Simulation Type	Relative Waste Acceptance Criteria						
	^{99}Tc	^{3}H	^{238}U	^{90}Sr	^{137}Cs	^{129}I	^{113}Cd
1D	0.998	0.979	0.989	0.993	0.996	0.996	0.988
2D	0.841	0.839	0.884	0.947	0.960	0.982	0.879

Table 3.5 shows the vertical water flux through the cementitious waste source for the grout and sand backfill material. The difference in flux through the source was small (≤ 0.025 mm/yr), demonstrating that the cement hydraulic properties control the vertical water flux. Two-dimensional fluxes were approximately 30 percent lower than one-dimensional simulations, again associated with the presence of flow in the second dimension.

Table 3.5. Water Flux Through the Contaminant Source for Sand- Versus Grout-Filled Monoliths

Simulation Case	Water Flux Through Source (mm/yr)
Case 1: 1D Grout	0.511
Case 2: 1D Sand	0.524
Case 3: 2D Grout	0.351
Case 4: 2D Sand	0.376

3.1.2 Distribution Coefficient (K_d) and Half-Life Sensitivity Analysis

Because of uncertainties associated with the distribution coefficient (K_d) and half-life, simulations were run that explored the sensitivity of the waste acceptance criteria to the selected K_d and half-life. The simulations were identical to Case 1, except that hypothetical radionuclides were considered that ranged in K_d from 0 to 1 mL/g and in half-lives from 30 to $1x10^{20}$ years. The K_ds considered were assumed to be the same for all materials. Figure 3.4 shows the maximum loading capacity as a function of K_d and half-life. The K_d has a very strong effect on the maximum loading capacity, varying from 7 to 10 orders of magnitude over the K_d range examined (0–1 mL/g). Maximum loading capacity is also shown to be dependent on radionuclide half-life; shorter half-lives result in larger maximum capacity estimates.

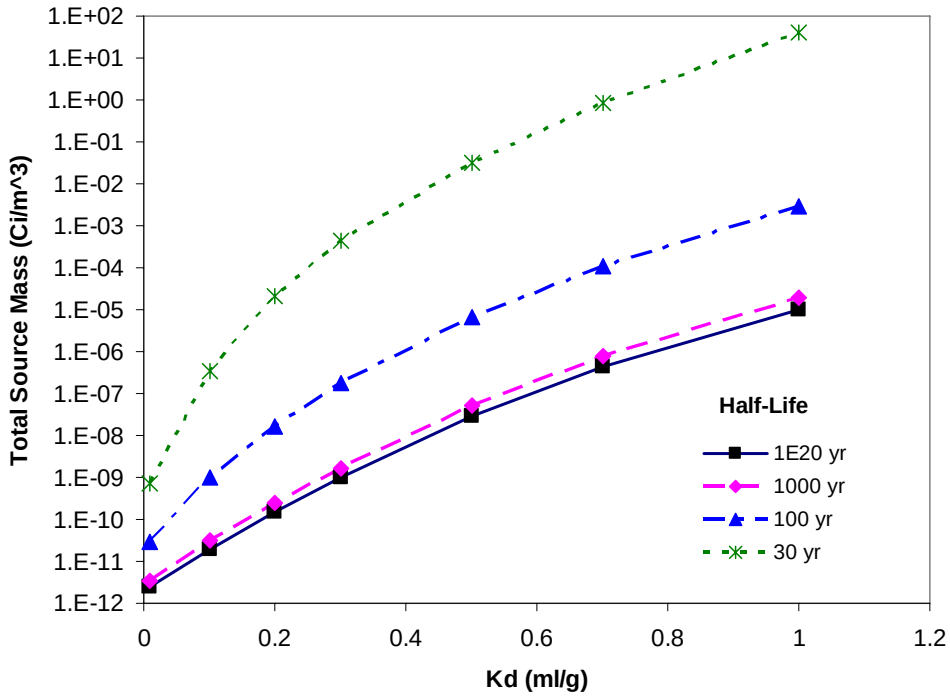

Figure 3.4. Estimated Maximum Loading Capacity as a Function of K_d and Half-Life

The effect of half-life on maximum loading capacity estimates is particularly significant as the K_d increases, with the difference in estimated maximum loading capacities for a radionuclide with a half-life of 30 and $1x10^{20}$ years increasing from 2 to 6 orders of magnitude. The sensitivity of estimated loading capacities to K_d and half-life suggests that uncertainties in assigned K_d and half-life values may introduce order of magnitude uncertainties in the estimated maximum loading capacities.

3.1.3 Recharge Sensitivity Analysis

For Cases 1, 2, 3, and 4 the first 10 years of the simulation period was ascribed a surface recharge of 43.1 mm/yr, followed by a decreased surface flux of 3.2 mm/yr over the 221-U structure for the remaining 990 years of the simulation. A sensitivity simulation was run to explore the effects on the acceptance criteria if the recharge was 100 mm/yr (a maximum bounding estimate) during the first 10 years of the simulation period. The simulation was identical to Case 3 in all aspects except recharge, which was set to 100 mm/yr from the beginning of the simulation to year 10. As with Case 3, from years 10–1,000, the recharge over the barrier of the 221-U Building was 3.2 mm/yr, while the recharge adjacent to the 221-U Building did not change (100 mm/yr). Figure 3.5 shows the resulting steady-state flow fields for Case 3 (43.1 mm/yr recharge) and Case 3b (100 mm/yr recharge). Higher saturation conditions exist in the sediment outside the barrier as a result of the higher recharge rates. In the 221-U Building the saturations under both recharge conditions remained nearly identical. Flow patterns from the elevated recharge case show little departure from Case 3.

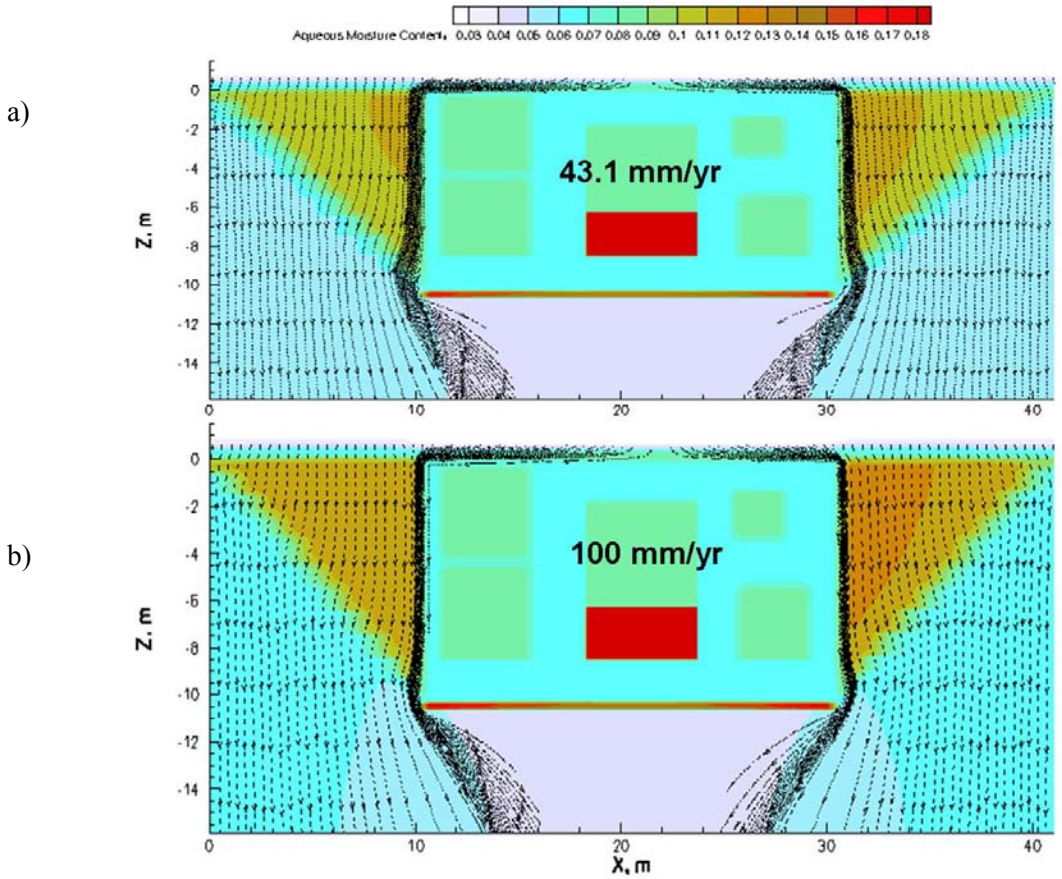

Figure 3.5. Flow Fields for a) 43.1 (Case 3) and b) 100 mm/yr (Case 3b) Scenarios

The steady-state vertical water fluxes across a horizontal plane that runs through the center of the source are shown in Figure 3.6 for the 43.1 and 100 mm/yr scenarios. The largest flux difference occurred in the sediment surrounding the 221-U Building, with the water flux along the outside walls of the structure being over 250 mm/yr greater under the 100 mm/yr scenario. Water flux through the source increased by 0.03 mm/yr.

a)

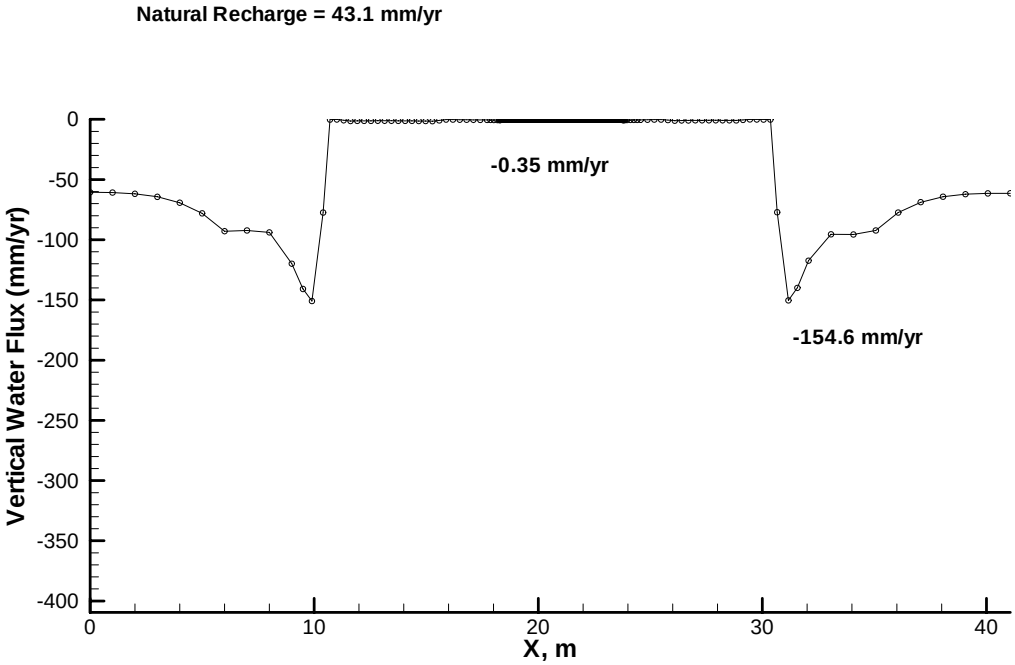

b)

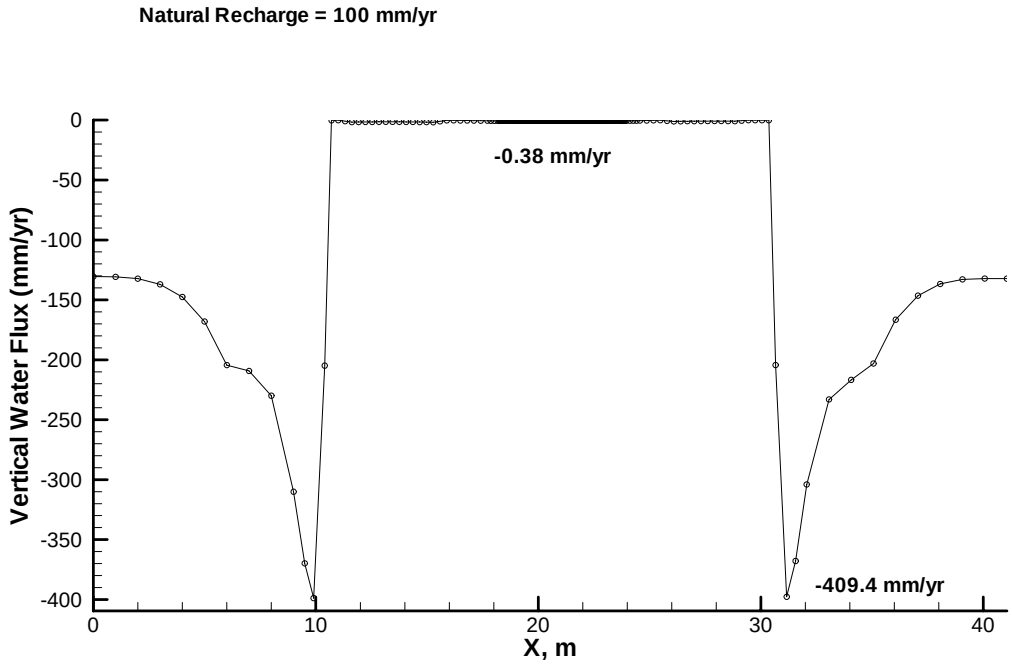

Figure 3.6. Vertical Water Flux Through Horizontal Plan for a) 43.1 (Case 3) and b) 100 mm/yr (Case 3b) Scenarios. Horizontal plane goes through center of source.

The maximum loading capacities for a recharge rate of 100 mm/yr range from 87 to 99% of the maximum loading capacities estimated for a recharge rate of 43.1 mm/yr (Table 3.6). The largest decrease in maximum loading capacity is associated with the conservative species ^{99}Tc and ^{3}H. As dictated by the release model, more ^{99}Tc and ^{3}H mass is released and available for transport earlier in the simulation when the elevated recharge rate has a greater effect on transport behavior.

Table 3.6. Waste Acceptance Criteria and Relative Waste Acceptance Criteria (Case 3b Loading Capacity/Case 3 Loading Capacity) for 100 mm/yr (Case 3b) Recharge Scenario

Simulation Case	Waste Acceptance Criteria (Ci/m^3)						
	^{99}Tc	^{3}H	^{238}U	^{90}Sr	^{137}Cs	^{129}I	^{113}Cd
Case 3b (100 mm/yr)	5.47E-09	3.43E-05	4.17E+43	1.01E+05	3.36E+08	1.06E+10	1.38E+54
Relative Waste Acceptance Criteria							
Case 3b (100 mm/yr)	0.870	0.872	0.911	0.959	0.968	0.989	0.905

3.2 Flow, Heat, and Solute Transport (STOMP-WAE) Results

The STOMP-WAE simulations examined the impact of thermal loading on establishing the waste acceptance criteria. For the STOMP-WAE simulations the source was assigned a constant temperature of approximately 150°F (65°C). Solution convergence issues required that the node spacing used for the STOMP-WAE simulations be coarser throughout the source region than those used for the STOMP-W and STOMP-W-R simulations. To eliminate impacts to results that may occur due to changes in the simulation grid, STOMP-W simulations were also executed using the identical coarse grid for comparison with the STOMP-WAE results. Hence, STOMP-WAE results are reported as relative to STOMP-W results. Waste acceptance criteria using STOMP-WAE were estimated for the scoping one-dimensional cases and two-dimensional grout case described in Table 3.7.

The one-dimensional STOMP-WAE scoping simulations show that grout and sand backfill materials have similar maximum loading capacities, with the maximum difference in contaminant loading for the conservative species. This same behavior was estimated by the STOMP-W simulations and indicates that the effect of the process cell backfill material is not significant for establishing waste acceptance criteria. Hence, only the grout-filled monolith was simulated in two dimensions.

The calculated waste acceptance criteria for the STOMP-WAE cases and relative waste acceptance criteria are presented in Table 3.8. Results are presented as relative loadings to the waste acceptance criteria established with the base case flow and solute transport simulations (STOMP-W).

Table 3.7. STOMP-WAE Simulation Scenarios

Case	Scenario
1	**1-D** Simulation; top 2/3 of the process cell was filled with **grout**; bottom 1/3 of the process cell contained the cementitious waste form; natural recharge = 43.1 mm/yr
2	**1-D** Simulation; top 2/3 of the process cell was filled with **sand**; bottom 1/3 of the process cell contained the cementitious waste form; natural recharge = 43.1 mm/yr
3	**2-D** Simulation; top 2/3 of the process cell was filled with **grout**; bottom 1/3 of the process cell contained the cementitious waste form; natural recharge = 43.1 mm/yr

Table 3.8. STOMP-WAE Waste Acceptance Criteria and Waste Acceptance Criteria Relative to STOMP-W (Base Case) Simulations

Simulation Case	Waste Acceptance Criteria (Ci/m^3)						
	^{99}Tc	^{3}H	^{238}U	^{90}Sr	^{137}Cs	^{129}I	^{113}Cd
Case 1: 1D Grout	9.12E-10	6.10E-07	9.52E+35	2.88E+04	3.73E+07	1.63E+09	1.24E+44
Case 2: 1D Sand	1.09E-09	5.08E-07	1.10E+36	2.57E+04	3.64E+07	1.85E+09	1.43E+44
Case 3: 2D Grout	1.41E-09	2.81E-06	1.63E+36	5.64E+04	1.94E+08	2.74E+09	2.12E+44
Relative Waste Acceptance Criteria							
Case 1: 1D Grout	0.463	0.068	6.75E-08	0.446	0.496	0.239	2.73E-10
Case 2: 1D Sand	0.554	0.058	7.92E-08	0.401	0.486	0.272	3.21E-10
Case 3: 2D Grout	0.223	0.071	3.57E-08	0.535	0.560	0.256	1.39E-10

The one-dimensional STOMP-WAE scoping simulations estimate maximum loading for the conservative species ^{99}Tc and ^{3}H as extremely small, less than 10^{-5} Ci/m^3. Like the STOMP-W simulations, the low waste acceptance criteria for ^{99}Tc and ^{3}H suggest that these radionuclides cannot be safely sequestered in the 221-U structure. The maximum loading capacity for moderately reactive species varied from 10^{4} Ci/m^3 for ^{90}Sr to 10^{9} for ^{129}I. Loading of the highly reactive species ^{238}U and ^{113}Cd exceeded 10^{35} Ci/m^3 and exceed known inventories at the Hanford Site.

The mass (activity) fractions of the contaminants are presented in Figures 3.7 and 3.8 at 1000 years for both the one- and two-dimensional simulations. Similar to the STOMP-W final contaminant distributions, both figures demonstrate the majority of contaminants still within the source area after 1000 years of simulation. Enhanced transport of the conservative species, ^{99}Tc and ^{3}H, is observed by the larger activity fractions in the layers adjacent and downstream of the source. A higher fraction of the solutes with K_d values in the mid-range (e.g., ^{90}Sr, ^{129}I and ^{137}Cs) is observed in the materials adjacent to the source relative to the STOMP-W (no heat impact) simulations. A comparison of the one- and two-dimensional grout-filled scenarios also shows a wider distribution of the contaminants in two dimensions. For all simulations, volatilized ^{3}H did not exit the upper surface of 221-U Building.

STOMP-WAE estimated maximum loading values were all less than maximum loading values estimated by STOMP-W. STOMP-WAE relative maximum loading values range from a low of 1.39E-10 for ^{113}Cd to 0.56 for ^{137}Cs. The reduction in maximum loading for ^{3}H can be attributed to the consideration of ^{3}H vapor transport in the STOMP-WAE simulations. Except for the highly reactive species, all remaining radionuclide maximum loading capacities were 2–4 times the estimates established with the STOMP-W, due to temperature impacts on diffusive transport and saturated hydraulic conductivities. For the highly reactive species ^{238}U and ^{113}Cd, the maximum loading capacities remained extremely large, and differences were not significant for establishing waste acceptance criteria.

A comparison of one-and two-dimensional simulation results (Table 3.9) for grout demonstrates that the maximum loading capacity is calculated to be larger in the two-dimensional simulations than in the one-dimensional conceptual model. The absence of contaminant spreading in the second dimension contributes to reduced maximum loading capacities in the one-dimensional simulations. For grout, the two-dimensional loading was on average approximately 2.6 times the one-dimensional maximum loading capacity.

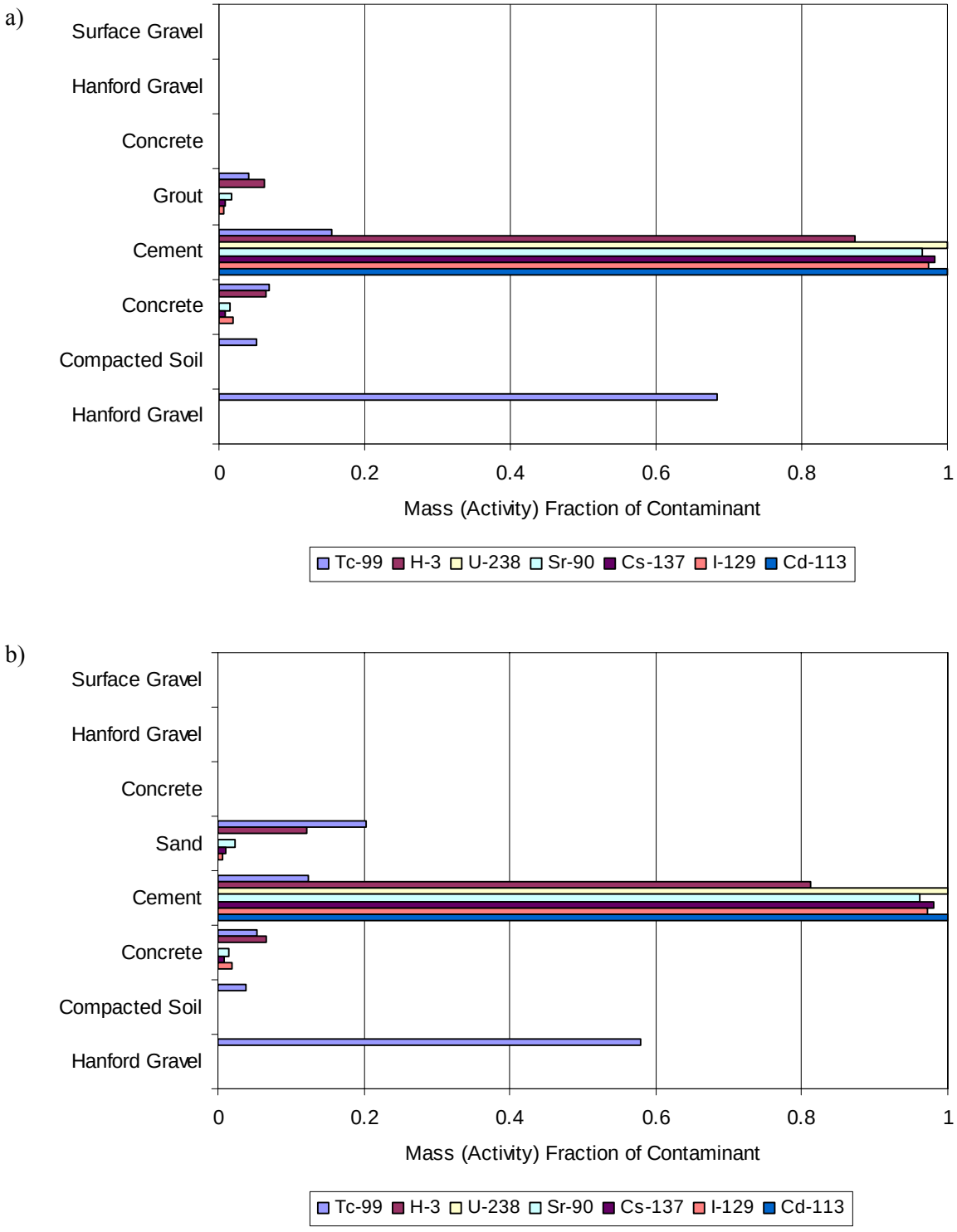

Figure 3.7. Mass Fraction of Contaminants for 1-D Model After 1000 Years of Simulation for Flow, Heat and Solute Transport (STOMP-WAE) for a) Grouted and b) Sand-Filled Monoliths

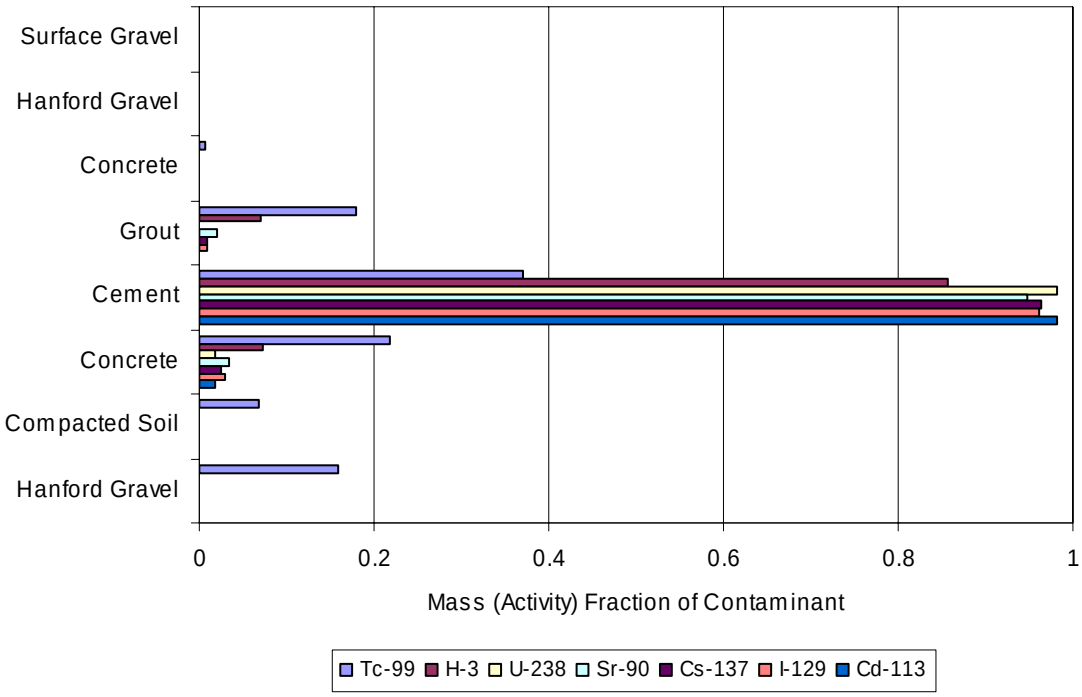

Figure 3.8. Mass (Activity) Fraction of Contaminants For Two-Dimensional Model After 1000 Years of Simulation for Flow, Heat and Solute Transport (STOMP-WAE) for Grouted Monolith

Table 3.9. Relative Loading Capacity (2-D/1-D Loading Capacity) for Grout-Filled Monolith

	Relative Waste Acceptance Criteria						
Fill Material	^{99}Tc	^{3}H	^{238}U	^{90}Sr	^{137}Cs	^{129}I	^{113}Cd
Grout	1.541	4.603	1.716	1.960	5.215	1.676	1.717

For the STOMP-WAE simulations, neither backfill material consistently allowed for larger loading capacities (Table 3.10). On average, sand allowed for loading capacities approximately 1.05 times that of grout.

Table 3.10. Relative Loading Capacity for Sand- Versus Grout-Filled Monolith

	Relative Waste Acceptance Criteria						
Simulation Type	^{99}Tc	^{3}H	^{238}U	^{90}Sr	^{137}Cs	^{129}I	^{113}Cd
1D	1.195	0.834	1.160	0.892	0.976	1.135	1.160

The relationship between one- and two-dimensional calculated water flux through the source (Table 3.11) was similar to that estimated by STOMP-W, with the one-dimensional water flux being higher than two-dimensional water flux. The estimated STOMP-W and STOMP-WAE water fluxes were very similar, differing by less than 0.04 mm/yr.

Table 3.11. Water Flux Through the Contaminant Source for Sand- and Grout-Filled Monoliths

Simulation Case	Water Flux Through Source (mm/yr)
Case 1: 1D Grout	0.518
Case 2: 1D Sand	0.531
Case 3: 2D Grout	0.312

3.3 Flow, Solute and Reactive Transport (STOMP-W-R) Results

The STOMP-W-R simulations examined the effect that precipitation/dissolution reactions had on establishing the waste acceptance criteria by modifying the porosity as changes in mineral volumes occurred. Changes in the porosity affected both the diffusion release rate and the diffusional transport through the altered porous media. The results presented in this section are intended to demonstrate the potential that aqueous-solid phase reactions can have on establishing the waste acceptance criteria, but by no means quantify an absolute loading. Too many unknowns exist with respect to kinetic reaction rates, heat effects, and secondary mineral precipitates. Even the cementitious waste formulation is unknown.

Although several minerals were identified as potential secondary mineral precipitates, only three of the minerals (illite, sepiolite and clinochlore-14A) identified precipitated in the cement waste form during the 1000 year simulation. Ettringite and jennite, minerals in the cement and concrete, reprecipitated in small amounts in the near-field materials. Because the C-S-H gel (jennite) mineral in the cement and concrete underwent dissolution, silica concentrations increased in the system. Despite this increase, minerals containing silica did not form in significant quantities. Further work is needed to identify potential mineral precipitates, particularly with respect to silica bearing minerals. Hence, reaction rates were set low (e.g., ~1 x 10^{-15} mol/m^2 s) to lower silica concentrations in the system. Although this limited the porosity changes to the cement waste form and near-field materials, the results still demonstrate the potential that precipitation/dissolution reactions may have on establishing waste acceptance criteria. The reactive transport modeling performed in this analysis should be considered a prototype for future assessments.

Only one-dimensional scoping calculations were carried out in this analysis (Table 3.12). Both grout- and sand-filled monoliths were simulated with a reactive cementitious waste form.

Table 3.12. STOMP-W-R Simulation Scenarios

Case	Scenario
1	1-D Simulation; top 2/3 of the process cell was filled with **grout**; bottom 1/3 of the process cell contained the cementitious waste form; natural recharge = 43.1 mm/yr
2	1-D Simulation; top 2/3 of the process cell was filled with **sand**; bottom 1/3 of the process cell contained the cementitious waste form; natural recharge = 43.1 mm/yr

3.3.1 Pore Water pH

The pore water pH initial condition and at 1000 years for the grouted monolith is shown in Figure 3.9a. This figure shows that at the start of the simulation, the pH of the soil materials is ~8, and the pH of the cement, grout, and concrete materials is ~10.5. According to Krupka and Serne (2001), as capability that can be used for future performance predictions once site-specific data are obtained.

a)

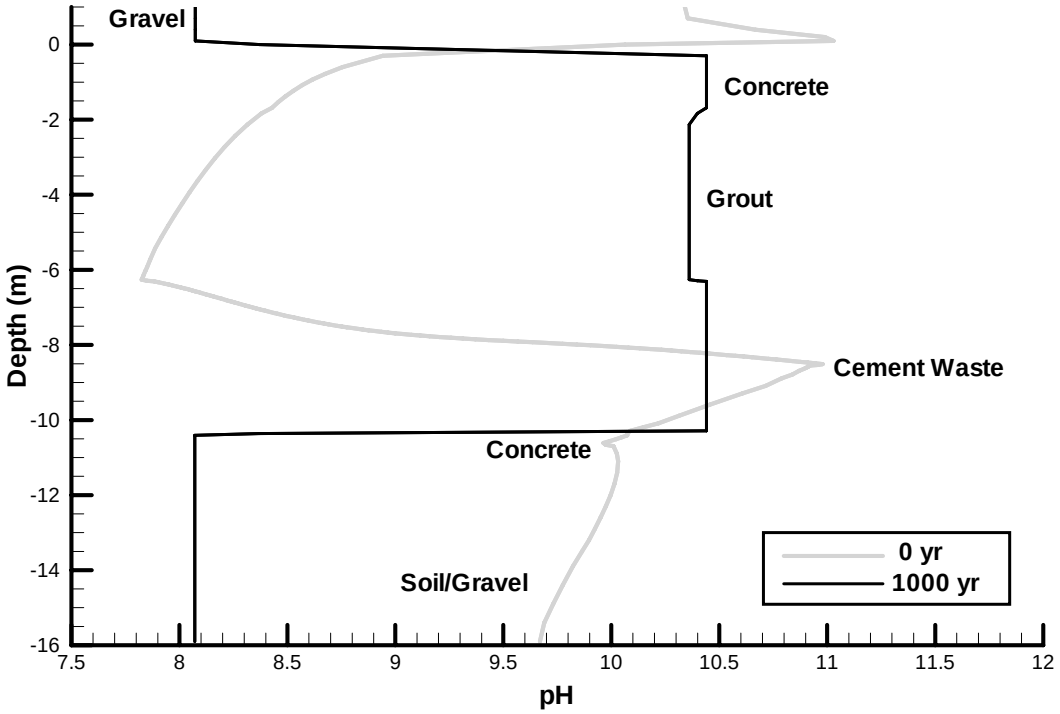

Figure 3.9a. Pore Water pH for Initial Condition and after 1000 yr Simulation for Grouted Monolith

b)

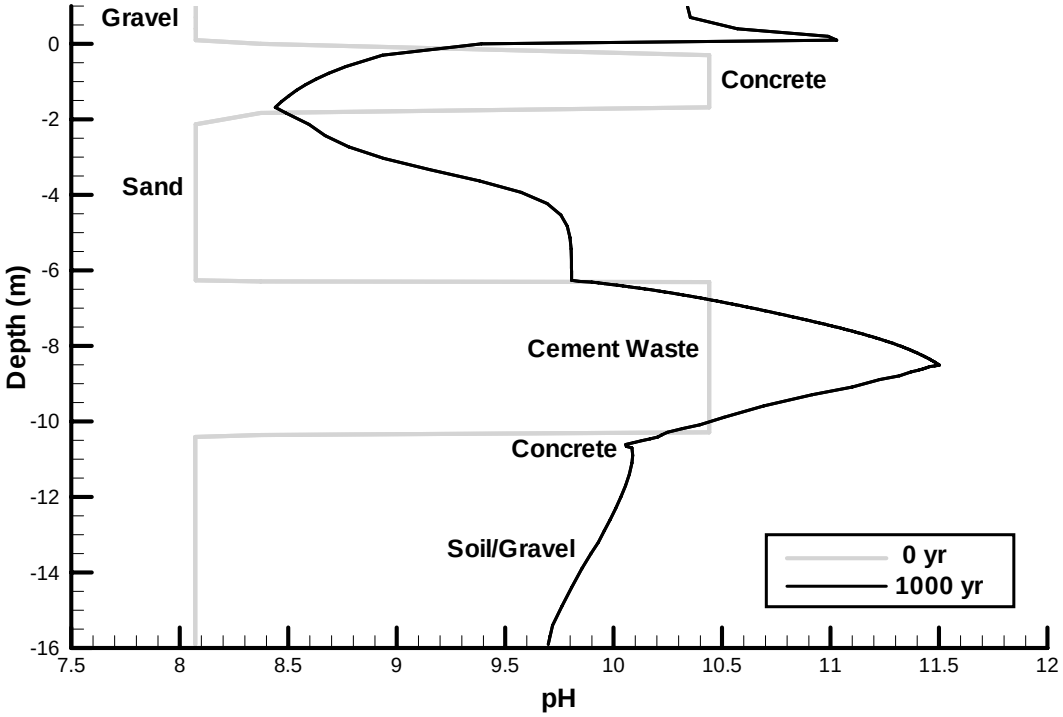

Figure 3.9b. Pore Water pH for Initial Condition and after 1000 yr Simulation for Sand-Filled Monolith

The pH of the sand monolith is shown in Figure 3.9b for the initial condition and after 1000 years of simulation. The initial condition is the same as the initial condition for the grouted monolith, except the pH of the sand is the same as the other soil and gravel materials. Similar to the grouted monolith simulation, the pH at the center of the cement waste has increased by an order of magnitude, but has a lower pH near the adjacent sand and concrete materials. Because the sand used to backfill the process cell maintains a higher pH relative to the grout-filled monolith, the peak pH of the cement waste is a half-order of magnitude higher.

The pH distribution for both profiles may be suspect, as more buffering capacity would be expected for the engineered materials. Further work is required to investigate the behavior of the hypothetical formulations assumed in this analysis. The emphasis for the reactive transport simulations, however, is on the approach rather than the results. The reactive transport modeling demonstrates a reactive transport

3.3.2 Porosity Changes

The dissolution and precipitation reactions taking place in the subsurface materials resulted in mineral volume changes. Shown in Figure 3.10 is the percent difference in the porosity distribution between time zero and 1000 years of simulation for both the grouted and sand monoliths. In all materials except the cementitious waste form, the porosity increased, particularly in the materials downstream of the waste. In the cement, however, the porosity decreased, which affected both the diffusion release rate and the rate of diffusive transport. The effect on the diffusion release rate, however, was negligible (< 0.1%). Hence, a decrease in the diffusional transport rate caused a slower transport from the waste source, resulting in an increase in the waste acceptance criteria by an average of ~5%.

The waste acceptance criteria relative to the base case (STOMP-W) are shown for the one-dimensional cases with grout and sand backfill in Table 3.13. Results are presented as relative loadings to the waste acceptance criteria established with the base case flow and solute transport simulations (STOMP-W). The maximum loading was determined when the amount of contaminant exiting the 221-U Building exceeded 1 pCi/m^2 over the 1,000-year simulation period.

The mass (activity) fractions of the contaminants are presented in Figure 3.11 at 1000 years for the one-dimensional simulations. Given that the maximum loadings for the STOMP-W and STOMP-W-R simulations were similar, the final activity distributions for the STOMP-W-R simulations are similar to the final distributions obtained in the STOMP-W analysis. Both the grout- and sand-filled scenarios demonstrate the majority of contaminants still within the source area after 1000 years of simulation, and the enhanced transport of the conservative species, ^{99}Tc and ^{3}H, is observed by the larger activity fractions in the layers adjacent and downstream of the source.

a)

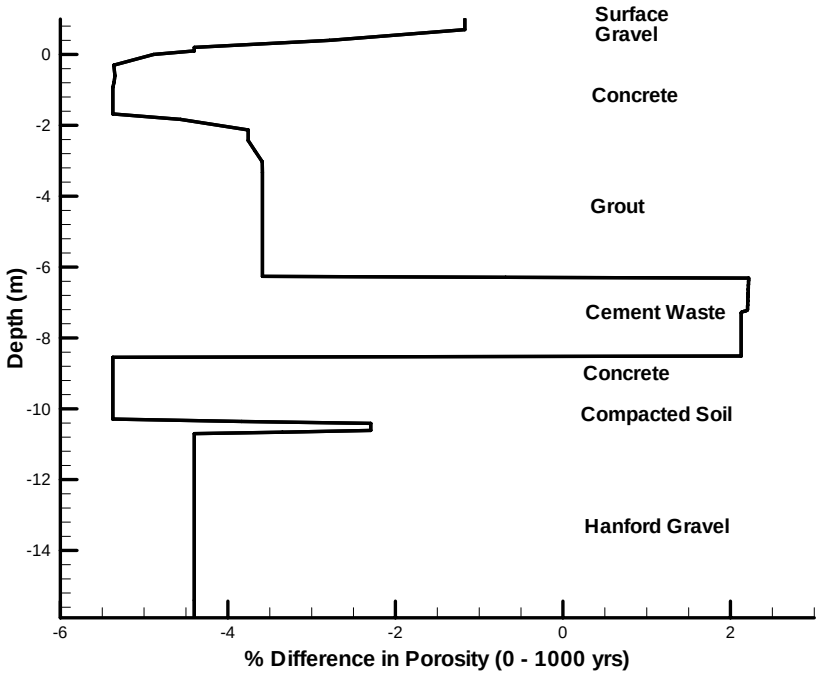

b)

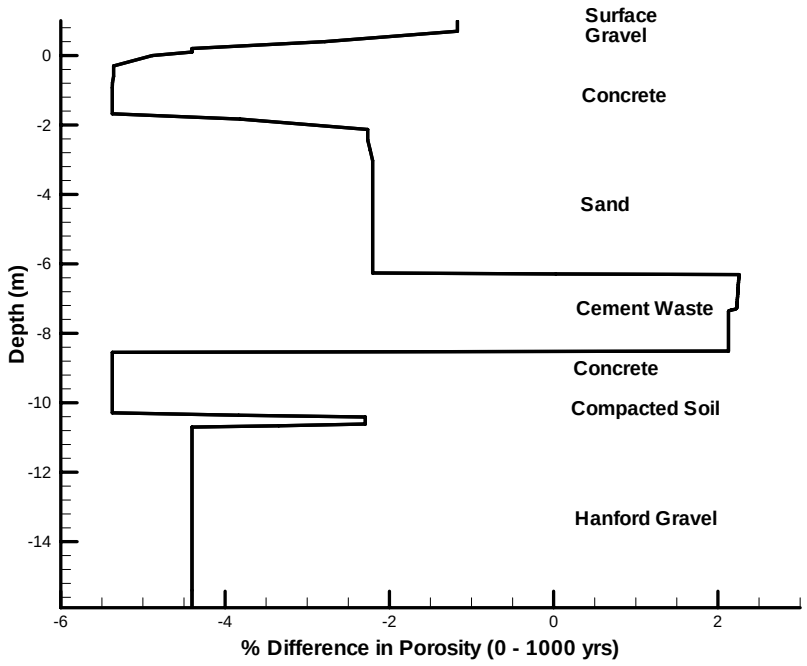

Figure 3.10. Porosity Changes over 1000-Yr Simulation Period for a) Grouted and b) Sand Monoliths

Table 3.13. STOMP-W-R Waste Acceptance Criteria and Waste Acceptance Criteria Relative to STOMP-W (Base Case) Simulations

Simulation Case	Waste Acceptance Criteria (Ci/m^3)						
	^{99}Tc	^{3}H	^{238}U	^{90}Sr	^{137}Cs	^{129}I	^{113}Cd
Case 1: 1D Grout	2.01E-09	7.20E-06	3.77E+41	7.69E+03	7.22E+06	3.36E+08	1.17E+52
Case 2: 1D Sand	2.54E-09	6.88E-06	3.46E+41	7.19E+03	6.75E+06	3.14E+08	1.08E+52
Relative Waste Acceptance Criteria							
Case 1: 1D Grout	1.017	1.061	1.053	1.046	1.042	1.042	1.053
Case 2: 1D Sand	1.016	1.070	1.061	1.049	1.046	1.049	1.061

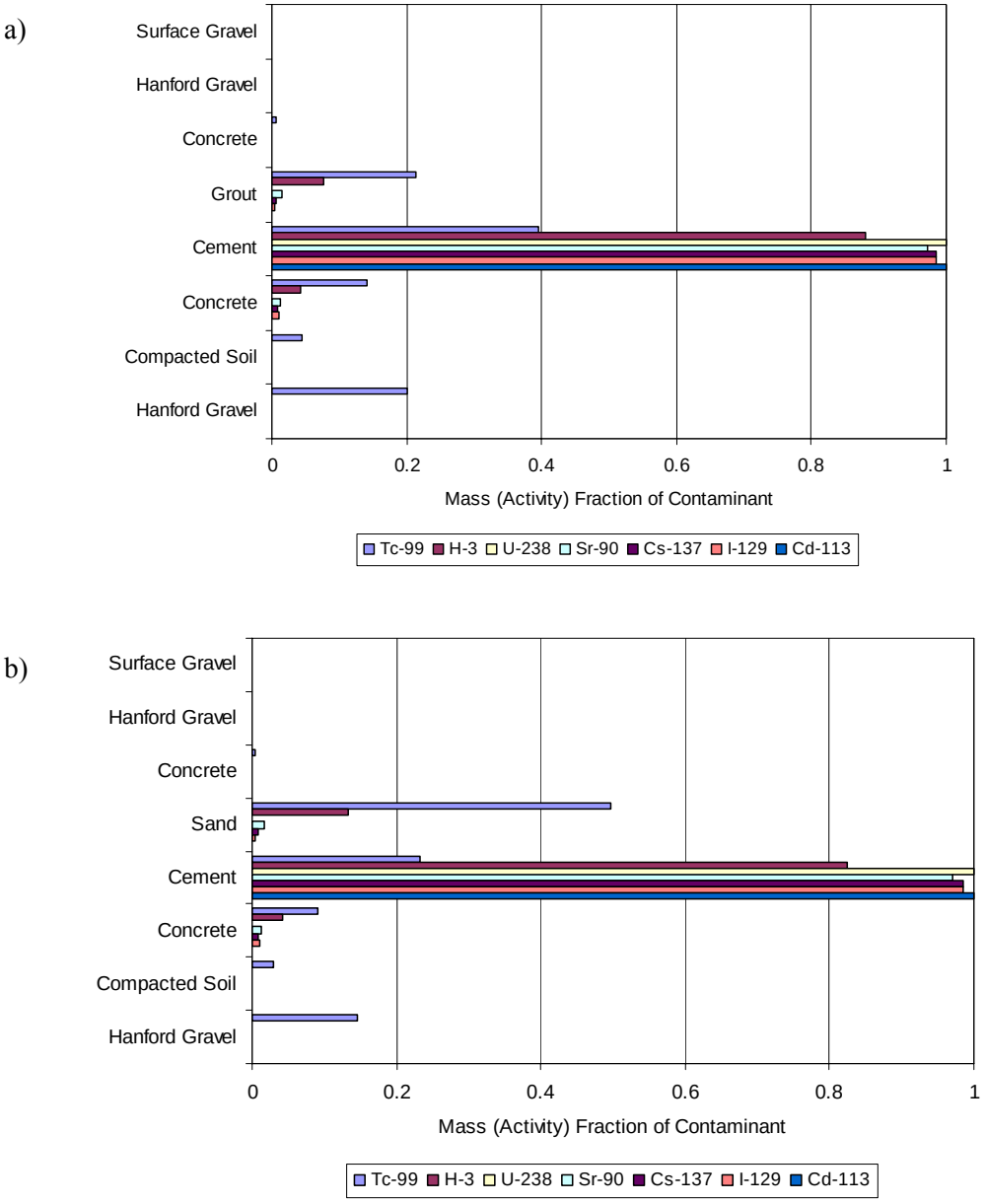

Figure 3.10. Mass Fraction of Contaminants for 1-D Model After 1000 yr Simulation for Flow and Solute Transport with Precipitation/Dissolution Reactions (STOMP-W-R) for a) Grouted and b) Sand-Filled Monoliths

4.0 Summary and Conclusions

Initial scoping calculations were performed in this investigation to establish waste acceptance criteria for contaminants sequestered in a cementitious waste form in the 221-U Building. The release and transport of seven contaminants, representing a range of sorption/desorption behavior and different half-lives, were assessed for a 1,000 year period for grout and sand monoliths. Specifically, simulations were executed to identify the maximum loading of contaminant activity (without respect to volume) that could be emplaced within the 221-U Building with no more than 1 pCi/m^2 of contaminant exiting the bottom of the structure within a 1,000 year time period.

It is important to emphasize that the waste acceptance criteria established in this report are based on several important assumptions that were used to carry out the analysis. These assumptions include

- No cracks or fissures in the grout, cement, or concrete.
- Non-site-specific data for the waste formulation and source release rates represented the potential waste streams at the 221-U Building
- No volume limitations on the mixture of the contaminant in the waste form.

Preferential flow in the engineered materials is likely, which could drastically limit the amount of contaminant that could be safely sequestered in the U-221 building. Apart from physical volume limitations, the form in which the contaminants are sequestered could have a profound impact on the source release rates. The defensibility of the waste acceptance criteria provided in this report can be determined once site-specific experimental data are acquired. While the current contaminant loading estimates satisfy the requirements for initial scoping calculations, a more defensible representation of source release rates, chemical interactions and transport behavior are required to reduce the uncertainty in the waste acceptance criteria for future performance assessments.

4.1 Modeling Approach

Three sets of simulations were used to assess geochemical processes, heat flow, and solute transport. In the first set, flow and solute transport simulations were executed to determine the maximum loading when heat impacts were considered negligible. The only chemical reaction considered was the use of a distribution coefficient (K_d) that assumed linear and reversible sorption. This set of simulations was considered a base case for determining the waste acceptance criteria because it accounted for primary processes likely controlling contaminant loading in the 221-U Building. In the other two sets, other potential factors that could affect the maximum contaminant loading in the building were examined. These waste acceptance criteria were reported relative to the base case, so that the effects of thermal loading and precipitation/dissolution reactions could be more easily discerned. The second set of simulations examined the effect of thermal loading on establishing the waste acceptance criteria, whereas a third set analyzed the potential impact precipitation/dissolution reactions could have on establishing waste acceptance criteria. In this set of simulations, thermal flow was not considered, and the effect elevated temperatures in the building might have on reaction rates was also ignored.

The simulations presented in this report are considered initial scoping calculations and, as such, have not fully integrated all of the potential processes into a single analysis. The results presented here demonstrated the importance of considering processes outside of the basic approach shown in the base case. At this stage, no data are available to do a more detailed analysis that fully integrates thermal and reactive transport. Hence, the approach presented in this report serves as a prototype for future modeling efforts that integrate both data and modeling to add technical defensibility to future performance predictions.

4.2 Results

Results of the simulations demonstrated that contaminants that are conservatively transported with water flow (e.g., ^{99}Tc and ^{3}H) cannot be safely sequestered in the 221-U Building using the waste stabilization approach used in this study. By contrast, nearly an infinite amount of contaminants that are moderately to strongly retarded (e.g., $K_d \geq 1.0$) can be sequestered. The amount of contaminants such as ^{238}U and ^{113}Cd that can be sequestered is likely limited by volume. For contaminants that are only slightly retarded (e.g., $0 < K_d < 1.0$), specific limits on waste acceptance were established, but it was demonstrated that the uncertainty in the K_d and half-life may introduce significant uncertainties in the estimated maximum loading capacities. For all contaminants, waste acceptance criteria were higher when the open galleries were backfilled with grout rather than sand.

A sensitivity analysis of the preclosure barrier recharge rate demonstrated only a small impact on the flux through the contaminant source and hence on the waste acceptance criteria. This was due to a surface gravel layer that permitted runoff to flow around the concrete structure of the 221-U Building.

Tables 4.1–4.3 summarize the results of the base case (STOMP-W) simulations and report the relative loading impact when additional processes are considered. The relative loading, for example, is the maximum loading determined for a contaminant in STOMP-WAE normalized by the loading for STOMP-W. Heat loading had a significant impact on the maximum loading, with maximum loading estimates for all contaminants, except ^{238}U and ^{113}Cd, decreasing by ~2–4 times the estimates when heat impacts were considered negligible. For the more strongly retarded species ^{238}U and ^{113}Cd, the estimates differed by several orders of magnitude. However, the maximum loading estimates were still so large that they exceed known inventories at the Hanford Site. Although contaminant densities were not considered, it is also likely that the loading estimates exceed the available storage volume in the 221-U Building.

The results demonstrate that consideration of reactive transport had a small impact on the establishing waste acceptance criteria. This occurred in part due to the early stage at which the reactive transport modeling has been developed thus far. For example, heat impacts on the K_d-based solute transport were not considered in the reactive transport simulations, although they are likely to have a larger impact on mineral solubilities (i.e., the contaminant release rate) and kinetic rates of reaction. Moreover, kinetic rates were set low in these initial scoping calculations because further work is required to identify potential secondary mineral precipitates. Even with slow kinetics, however, waste acceptance criteria increased on average by ~5%.

A more mechanistic approach for describing sorption/desorption will be needed once data on waste formulation are available. Potential chemical interactions among different contaminants will also need to be considered, as well as minerals that control the release of the different contaminants. This will add scientific defensibility to future performance assessments of the 221-U Building for waste sequestration.

Table 4.1. Waste Acceptance Criteria based on One-Dimensional Grout STOMP-W Simulations and Relative Loadings for Heat and Reactive Transport

STOMP Mode	Waste Acceptance Criteria (Ci/m^3)						
	Tc-99	H-3	U-238	Sr-90	Cs-137	I-129	Cd-113
W	1.97E-09	8.97E-06	1.41E+43	6.44E+04	7.52E+07	6.84E+09	4.52E+53
Relative Waste Acceptance Criteria							
WAE	0.463	0.068	6.75E-08	0.446	0.496	0.239	2.73E-10
W-R	1.017	1.061	1.053	1.046	1.042	1.042	1.053

Table 4.2. Waste Acceptance Criteria Based on One-Dimensional Sand STOMP-W Simulations and Relative Loadings for Heat and Reactive Transport

STOMP Mode	Waste Acceptance Criteria (Ci/m^3)						
	Tc-99	H-3	U-238	Sr-90	Cs-137	I-129	Cd-113
W	1.97E-09	8.78E-06	1.39E+43	6.40E+04	7.48E+07	6.81E+09	4.47E+53
Relative Waste Acceptance Criteria							
WAE	0.554	0.058	7.92E-08	0.401	0.486	0.272	3.21E-10
W-R	1.016	1.070	1.061	1.049	1.046	1.049	1.061

Table 4.3. Waste Acceptance Criteria Based on Two-Dimensional Grout STOMP-W Simulations and Relative Loadings for Heat Transport

STOMP Mode	Waste Acceptance Criteria (Ci/m^3)						
	Tc-99	H-3	U-238	Sr-90	Cs-137	I-129	Cd-113
W	6.29E-09	3.93E-05	4.58E+43	1.05E+05	3.47E+08	1.07E+10	1.52E+54
Relative Waste Acceptance Criteria							
WAE	0.223	0.071	3.57E-08	0.535	0.560	0.256	1.39E-10

5.0 References

Albenesius EL. 2001. *Computer Modeling of Saltstone Landfills by Intera Environmental Consultants*. DPST-83-529, Savannah River Site, Aiken, South Carolina.

Amiri O, A Ait-Mokhtar, and M Sarhani. 2005. *Advances in Cement Research*. 17(1):39–45.

Atkinson A and AK Nickerson. 1988. "Diffusion and Sorption of Cesium, Strontium, and Iodine in Water-Saturated Cement." *Nuclear Technology,* 81(1):100–113.

Atkinson A, NM Everitt, and RM Guppy. 1989. "Time Dependence of pH in a Cementitious Repository." *Scientific Basis for Nuclear Waste Management XII*, W Lutze and RC Ewing (eds.), Volume 127, pp. 439–446. Materials Research Society, Pittsburgh, Pennsylvania.

Bacon DH and BP McGrail. 2005. *Waste Form Release Calculations for the 2005 Integrated Disposal Building Performance Assessment*. PNNL-15198, Pacific Northwest National Laboratory, Richland, Washington.

Berner UR. 1992. "Evolution of pore water chemistry during degradation of cement in a radioactive waste repository." *Waste Management,* 12:201–219.

Bechtel Hanford Inc. (BHI). 1999. *Phase I Interim Characterization Report for the 221-U Canyon Disposition Initiative*. BHI-01292, Rev. 0, Bechtel Hanford, Inc. Richland, Washington.

Bradbury MH and FA Sarott. 1995. *Sorption Databases for the Cementitious Near-Field of a L/ILW Repository for Performance Assessment.* PSI Bericht Nr. 95-06, Paul Scherrer Institute, Wurenligen and Villigen, Switzerland.

Bradbury, MH, and LR Van Loon. 1998. *Cementitious Near-Field Sorption Data Bases for Performance Assessment of a L/ILW Repository in a Palfris Marl Host Rock*. CEM-94: Update I. PSI Bericht 98-01, Paul Scherrer Institut, Villigen PSI, Switzerland.

Cass A, GS Campbell, and TL Jones. 1984. "Enhancement of Thermal Water Vapor Diffusion in Soil." *Soil Sci. Soc. Am. J*., 48:25-32.

Chemistry Daily. 2007. Accessed April 19, 2007 at http://www.chemistrydaily.com/chemistry/Cadmium.

Criscenti LJ, RJ Serne, KM Krupka, and MI Wood. 1996. *Predictive Calculations to Assess the Long-Term Effect of Cementitious Materials on the pH and Solubility of Uranium(VI) in a Shallow Land Disposal Environment.* PNNL-11182, Pacific Northwest Laboratory, Richland, Washington.

Freedman VL, ZF Zhang, SR Waichler, and SK Wurstner. 2005. *2005 Closure Assessments for WMA-C Tank Farms: Numerical Simulations*. PNNL-15377, Pacific Northwest National Laboratory, Richland, Washington.

Galindez JM, J Molinero, J Samper and CB Yang. 2006. "Simulating concrete degradation processes by reactive transport models." *Journal Physique IV France,* 136:177–188.

Goni S, A Guerrero, and M.P. Lorenzo. 2006. "Efficiency of fly ash belite cement and zeolite matrices for immobilizing cesium." *Journal of Hazardous Materials*. B137:1608–1617.

Hespe ED. 1971. "Leach Testing of Immobilized Radioactive Waste Solids: A Proposal for a Standard Method." *Atomic Energy Review*, Vol. 9, pp. 195-207. International Atomic Energy Agency, Vienna.

Jacques ID. 2001. *Final Data Report for the 221-U Building Characterization.* BHI-01565 Rev. 0, Bechtel Hanford, Inc., Richland, Washington.

Kemper WD and JC van Schaik. 1966. "Diffusion of salts in clay-water systems." *Soil Sci. Am. Proc*., 30:534-540.

Khaleel R and M.P. Connelly. 2003. *Modeling Data Package for an Initial Assessment of Closure for S-SX Tank Farm*. RPP-17209 Rev. 0, CH2M HILL Hanford Group, Inc., Richland, Washington.

Kincaid CT, JA Voodg, JW Shade, JH Westsik Jr, GA Whyatt, MD Freshley, MG Piepho, KA Blanchard, K Rhoads, and BG Lauzon. 1995. *Performance assessment of grouted double-shell tank waste disposal at Hanford.* WHC-SD-WM-EE-004 Rev. 1, Westinghouse Hanford Company, Richland, Washington.

Krupka KM and RJ Serne. 1998. *Effects on Radionuclide Concentrations by Cement/Groundwater Interactions in Support of Performance Assessment of Low-Level Radioactive Waste Disposal Facilities*. NUREG/CR-6377 (PNNL-11408), Pacific Northwest National Laboratory, Richland, Washington.

Krupka KM and RJ Serne. 2001. *Radionuclide Kd Values for Cementitious Systems*. PNWD-3127, prepared for the Italian National Agency for New Technology, Energy, and Environment (ENEA), Rome, Italy, by Battelle – Pacific Northwest Division, Richland, Washington.

Last GV, GW Gee, EJ Freeman, WE Nichols, KJ Cantrell, BN Bjornstad, MJ Fayer, DG Horton. 2006 *Vadose Zone Hydrogeology Data Package for Hanford Assessments*. PNNL-14702 Rev.1, Pacific Northwest National Laboratory, Richland, Washington.

Mualem Y. 1976. "A New Model for Predicting the Hydraulic Conductivity of Unsaturated Porous Media." *Water Resources Research*, 12:513-522.

Rockhold, ML, MJ Fayer, and PR Heller. 1993. *Physical and hydraulic properties of sediments and engineered materials associated with grouted double-shell tank waste disposal at Hanford*. PNL-8813, Pacific Northwest Laboratory, Richland, Washington.

Rockhold ML, MD White, and EJ Freeman. 2004. *Canyon Disposal Initiative - Numerical Modeling of Contaminant Transport from Grouted Residual Waste in the 221-U Building (U Plant)*. PNNL-14908, Pacific Northwest National Laboratory, Richland, Washington.

Savage D, D Noy, and M Mihara. 2002. "Modelling the interaction of bentonite with hyperalkaline fluids." *Applied Geochemistry*. 17:207–233.

Sposito G. 1989. *The Chemistry of Soils*. Oxford University Press, New York.

Steefel CI. 2001. *GIMRT: Software for modeling multicomponent, multidimensional reactive transport. Version 1.2. User's guide*. UCRL-MA-143182. Lawrence Livermore National Laboratory, Livermore, California.

Steefel CI and SB Yabusaki. 1996. *OS3D/GIMRT: Software for multicomponent–multidimensional reactive transport: User's manual and programmer's guide*. PNL-11166, Pacific Northwest National. Laboratory, Richland, Washington.

Trotignon L, H Peycelon, and X Bourbon. 2006. "Comparison of performance of concrete barriers in a clayey geological medium." *Physics and Chemistry of the Earth,* 31:610–617.

U.S. Department of Energy (DOE). 1998. P*hase I Feasibility Study for the Canyon Disposition Initiative (221-U Building)*. DOE/RL-91-11, Rev. 1, DOE Richland Operations Office, Richland, Washington.

U.S. Environmental Protection Agency (EPA). 2006. "Fact Sheets on Commonly Encountered Radionuclides." Accessed April 19, 2007, at http://www.epa.gov/radiation/radionuclides.

van Genuchten MTh. 1980. "A closed-form equation for predicting the hydraulic conductivity of unsaturated soils." *Soil Sci. Soc. Am. J.,* 44:892-898.

White MD and BP McGrail. 2005. *STOMP Subsurface Transport Over Multiple Phases Version 1.0 Addendum: ECKEChem Equilibrium-Conservation-Kinetic Equation Chemistry and Reactive Transport*. PNNL-15482, Pacific Northwest National Laboratory, Richland, Washington.

White MD and M Oostrom. 2000. *STOMP Subsurface Transport Over Multiple Phases Version 2.0 Theory Guide*. PNNL-12030, Pacific Northwest National Laboratory, Richland, Washington.

White MD and M Oostrom. 2006. *STOMP Subsurface Transport Over Multiple Phases Version 4.0 User's Guide*. PNNL-15782, Pacific Northwest National Laboratory, Richland, Washington.

Zhang ZF and Y Xie. 2005. *Numerical Modeling of Contaminant Transport from Grouted Residual Waste in the 221-U Building (U Plant)*. PNNL-15261, Pacific Northwest National Laboratory, Richland, Washington.

Zhang ZF, VL Freedman, and MD White. 2003. *2003 Initial Assessments of Closure for the C Tank Farm Field Investigation Report (FIR):Numerical Simulations*. PNNL-14334, Pacific Northwest National Laboratory, Richland, Washington.

Zhang ZF, VL Freedman, SR Waichler, and MD White. 2004. *2004 Initial Assessments of Closure for the S-SX Tank Farm: Numerical Simulations*. PNNL-14604, Pacific Northwest National Laboratory, Richland, Washington.

Appendix A

Hydraulic and Thermal Properties

Appendix A: Hydraulic and Thermal Properties

Table A.1. Physical and Hydraulic Properties of Sediments and Engineered Materials for the 221-U Building Model Domain (Sr was calculated using Sr = θr/θs)

Geologic Unit	ρ_p (g/cm^3)	θ_s (cm/cm^3)	K_s (cm/s)	α (cm^{-1})	n (-)	θ_r (cm/cm^3)	S_r (-)
Surface Gravel[a]	2.8	0.518	1.85	3.54	2.66	0.014	0.027
Concrete[b]	2.63	0.067	1.33E-9	3.87E-5	1.29	0	0
Grout	2.63[d]	0.087[d]	1.47E-8[c]	1.08E-5[c]	1.65[c]	0[c]	0
Cement	2.7[e]	0.1839[f]	3.75E-10[e]	7.61E-6[e]	1.393[e]	0[e]	0
Compacted Soil[g]	2.72	0.353	1.80E-6	0.0121	1.37	0.0035	0.0099
Backfill[h]	2.76	0.316	1.91E-3	0.035	1.72	0.049	0.155
Hanford Gravel[i]	2.23	0.154	1.48E-3	0.0165	1.745	0.027	0.172
Sand	2.64	0.356	3.67E-5	0.0102	2.177	0.042	0.118

(a) Meyer and Serne (1999), Table 4.19 (Diversion Layer Gravel).
(b) Meyer and Serne (1999), Table 4.19 (Vault Concrete).
(c) Rockhold et al. (1993), Table 4.1 (DSSF Grout).
(d) Rockhold et al. (2004), Page 6.
(e) Rockhold et al. (1993), Table 4.1 (Concrete).
(f) Amiri et al. (2005).
(g) Meyer and Serne (1999), Table 4.19 (Compacted Silt Loam).
(h) Meyer and Serne (1999), Table 4.19 (Backfill).
(i) Last et al. (2006) (Appendix A, Template 200S-X, page A.22).

Table A.2. Parameters for Calculating Aqueous-Phase Diffusion Coefficient

Geological Units	Radionuclide	$D_{ab}^{(a)}$ (cm^2/s)	$a^{(a)}$ (-)	$b^{(a)}$ (-)
Backfill, Hanford Gravel, Compacted Soil, Sand	Tc-99	2.5E-05	0.005	10
	H-3	2.5E-05	0.005	10
	U-238	2.5E-05	0.005	10
	Sr-90	2.5E-05	0.005	10
	Cs-137	2.5E-05	0.005	10
	I-129	2.5E-05	0.005	10
	Cd-113	2.5E-05	0.005	10
Surface Gravel	Tc-99	1.0E-10	1	0
	H-3	1.0E-10	1	0
	U-238	1.0E-10	1	0
	Sr-90	1.0E-10	1	0
	Cs-137	1.0E-10	1	0
	I-129	1.0E-10	1	0
	Cd-113	1.0E-10	1	0
Concrete	Tc-99	5.0E-8	1	0
	H-3	5.0E-8	1	0
	U-238	5.0E-8	1	0
	Sr-90	5.0E-8	1	0
	Cs-137	5.0E-8	1	0
	I-129	5.0E-8	1	0
	Cd-113	5.0E-8	1	0
Grout	Tc-99	1.0E-6	1	0
	H-3	1.0E-6	1	0
	U-238	1.0E-6	1	0
	Sr-90	1.0E-6	1	0
	Cs-137	1.0E-6	1	0
	I-129	1.0E-6	1	0
	Cd-113	1.0E-6	1	0
Cement	Tc-99	5.21E-07	1	0
	H-3	5.21E-07	1	0
	U-238	4.58E-11	1	0
	Sr-90	2.20E-08	1	0
	Cs-137	4.21E-08	1	0
	I-129	4.54E-09	1	0
	Cd-113	1.15E-11	1	0
(a) Kincaid et al. (1995), Tables 3.14 and 3.15.				

Table A.3. Thermal Properties of Sediments and Engineered Materials for 221-U Building Model Domain[(a)]

Geologic Unit	Cass Model Parameter					Specific Heat
	a (W/m C)	b (W/m C)	c (-)	d (W/m C)	e (-)	(J/kg C)
Surface Gravel	42.7	18.8	5.315	222.6	-0.638	8.8
Hanford Gravel2	42.7	18.8	5.315	222.6	-0.638	8.8
Concrete	0.427	0.188	5.315	2.226	-0.638	880
Grout	0.427	0.188	5.315	2.226	-0.638	880
Cement	0.427	0.188	5.315	2.226	-0.638	880
Compacted Soil	4.33	-0.797	1.244	0.235	1.067	730.6
Hanford Gravel	0.427	0.188	5.315	2.226	-0.638	880

(a) Ward AL and JM Keller. Hydrology and Vegetation Data Package for 200-UW-1 Waste Site Engineered Surface Barrier Design (Unpublished.). PNNL-15464, Pacific Northwest National Laboratory, Richland, Washington.

References

Amiri O, A Ait-Mokhtar, and M. Sarhani. 2005. "Tri-dimensional modeling of cementitious materials permeability from polymodal pore size distribution obtained by mercury intrusion porosimetry tests." *Advances in Cement Research,* 17(1)39–45.

Kincaid CT, JA Voodg, JW Shade, JH Westsik Jr, GA Whyatt, MD Freshley, MG Piepho, KA Blanchard, K Rhoads, and BG Lauzon. 1995. *Performance assessment of grouted double-shell tank waste disposal at Hanford.* WHC-SD-WM-EE-004 Rev. 1, Westinghouse Hanford Company, Richland, Washington.

Last GV, GW Gee, EJ Freeman, WE Nichols, KJ Cantrell, BN Bjornstad, MJ Fayer, and DG Horton. 2006. *Vadose Zone Hydrogeology Data Package for Hanford Assessments*. PNNL-14702 Rev.1, Pacific Northwest National Laboratory, Richland, Washington.

Meyer PD and RJ Serne. 1999. *Near-field hydrology data package for the immobilized low-activity waste performance assessment*. PNNL-13035, Pacific Northwest National Laboratory, Richland, Washington.

Rockhold ML, MJ Fayer, and PR Heller. 1993. *Physical and hydraulic properties of sediments and engineered materials associated with grouted double-shell tank waste disposal at Hanford*. PNL-8813, Pacific Northwest Laboratory, Richland, Washington.

Rockhold ML, MD White, and EJ Freeman. 2004. *Canyon Disposal Initiative—Numerical Modeling of Contaminant Transport from Grouted Residual Waste in the 221-U Building (UPlant)*. PNNL-14908, Pacific Northwest National Laboratory, Richland, Washington.

Appendix B

Reactive Transport Properties

Appendix B: Reactive Transport Properties

Table B.1. Cement Waste Form Composition (based on Trotignon et al. 2006)

Mineral	Volume Fraction
Jennite	0.517
Portlandite	0.0328
Ettingite	0.0164
Monosulfoaluminate	0.1558
Hydrotalcite	0.0984

Table B.2. Grout Composition (based on Savage et al. 2002)

Mineral	Volume Fraction
Montmor-Na	0.2
Chalcedony	0.16
Calcite	0.03
Analcime	0.03
Quartz	0.18

Table B.3. Sand Composition

Mineral	Volume Fraction
Quartz	0.66
Calcite	0.01
Gypsum	0.01

Table B.4. Concrete Structure Mineralogical Composition (based on data found at http://www.ce.berkeley.edu/~paulmont/CE60New/cement.pdf)

Mineral	Mineral Volume Fraction
Jennite	0.1925
Portlandite	0.0770
Ettingite	0.0525
Monosulfoaluminate	0.0175
Hydrotalcite	0.0105
Quartz	0.6500

Table B.5. Soil Composition (compacted soil, Hanford gravel, and surface gravel) (based on Bacon and McGrail 2005)

Mineral	Mineral Volume Fraction
Albite_High	0.4
Illite	0.1
K-Feldspar	0.1
Quartz	0.4

Table B.6. Potential Secondary Mineral Precipitates

Cement	Grout	Sand
Tobermorite-14A	Gyrolite	SiO_2(am)
Clinochlore-14A	Illite	
Xonotlite	Saponite-Ca	
Sepiolite	Celadonite	
Katoite	Laumontite	
Foshagite		
Brucite		
Calcite		
SiO_2(am)		
Quartz		
Hillebrandite		
Gypsum		

Table B.7. Aqueous Species, Aqueous Reactions and Log Ks

Aqueous Species	
Al+++, CO2(aq), CO3--, Ca++,CaSO4(aq), H+,H2O, H2SiO4--,HCO3-,HSO4-,HSiO3-,K+,Mg++,Na+,OH-,SO4--,SiO2(aq),	
Aqueous Reactions	**Log K**
OH- + H+ = H2O	-13.999
HSO4- = H+ + SO4--	-1.9791
HSiO3- + H+ = H2O + SiO2(aq)	9.9525
H2SiO4-- + 2H+ = SiO2(aq) + 2H2O	22.9600
CaSO4(aq) = Ca++ + SO4--	-2.1111
CO3-- + H+ = HCO3-	10.3288
CO2(aq) + H2O = H+ + HCO3-	-6.3447

Table B.8. Boundary Condition: Total Concentrations for Infiltrating Rainwater

Aqueous Species	mol/L
Al+++	1.00E-10
Ca++	1.89E-05
H+	7.78E-06
H2O	55.508
HCO3--	3.15E-05
HSO4-	1.80E-05
K+	8.80E-06
Mg++	1.74E-05
Na+	9.58E-05
SiO2(aq)	4.71E-06

Table B.9. Solid Phase Reactions, Log Ks, Kinetic Reaction Rate and Specific Surface Area

Solid Phase Reactions	Log K	Kinetic Reaction Rate (mol/m^2 s)	Specific Surface Area (m^2/m^3)
Montmor-Na + 2H2O = 6OH- + 4SiO2(aq) + 0.33Na+ + 0.33Mg++ + 1.67Al+++	8.1489E+01	1.E-16	0.1
Chalcedony = SiO2(aq)	3.7344E+00	1.E-16	0.1
Calcite + H2O = OH- + HCO3- + Ca++	1.2137E+01	1.E-16	0.1
Analcime + 0.92H2O = 3.84OH- + HCO3- + 2.04SiO2(aq) + 0.96Na+ + 0.96Al+++	4.7599E+01	1.E-16	0.1
Quartz = SiO2(aq)	4.0056E+00	1.E-13	0.1
Portlandite = 2OH- + Ca++	5.4260E+00	1.E-16	0.05
Jennite = 18OH- + 9Ca++ + 6SiO2(aq) + 2H2O	1.0184E+02	1.E-16	0.05
Ettringite = 15OH- + 6Ca++ + 2Al+++ + 3HSO4- + 23H2O	1.4141E+02	1.E-17	0.05
Monosulfoalu = 13OH- + 4Ca++ + 2Al+++ + HSO4- + 5H2O	1.0891E+02	1.E-16	0.05
Hydrotalcite = 14OH- + 6Mg++ + 2Al+++ + 3H2O	1.2054E+02	1.E-17	0.05
Gypsum + H+ = Ca++ + HSO4- + 2H2O	2.5413E+00	1.E-07	0.1
SiO2(am) = SiO2(aq)	4.0702E+00	1.E-07	0.1
Tobermorite-14A = 10H- + 5Ca++ + 6SiO2(aq) + 5.5H2O	7.6100E+01	1.E-07	0.1
Clinochlore-14A +4H2O = 16OH- + 3SiO2(aq) + 5Mg++ + 2Al+++	1.5664E+02	1.E-07	0.1
Xonotlite + 5H2O = 12OH- + 6Ca++ + 6SiO2(aq)	1.5664E+02	1.E-07	0.1
Sepiolite = 8OH- + 6SiO2(aq) + 4Mg++ + 3H2O	8.1521E+01	1.E-07	0.1
Katoite = 12OH- + 3Ca++ + 2Al+++	8.8950E+01	1.E-07	0.1
Foshagite +2.5H2O = 8OH- + 4Ca++ + 3SiO2(aq)	4.6022E+01	1.E-07	0.1
Brucite = 2OH- + Mg++	1.1684E+01	1.E-07	0.1
Gyrolite = 4OH- + 2Ca++ + 3SiO2(aq) + 0.5H2O	3.3071E+01	1.E-07	0.1
Illite + 3H2O = 8OH- + 3.5SiO2(aq) + 0.6K+ +	1.0293E+02	1.E-13	0.1
Saponite-Ca + 2.66H2O = 7.32OH- + 0.17Ca++ +	7.6147E+01	1.E-07	0.1
Celadonite + 2H2O = 6OH- + 4SiO2(aq) + K+ + Mg++	7.6514E+01	1.E-07	0.1
Laumontite = 8OH- + Ca++ + 4SiO2(aq) + 2Al+++	9.8287E+01	1.E-07	0.1
Albite_high + 2H2O = 4OH- + 3SiO2(aq) + Na+ +	5.1900E+01	1.E-13	0.1
K-Feldspar + 2H2O = 4OH- + 3SiO2(aq) + K+ +	5.6259E+01	1.E-13	0.1

Table B.10. Concentration Initial Condition: Cementitious Waste Form

Aqueous Species	mol/L
Al+++	5.09E-28
Ca++	2.53E-03
H2O	55.508
HCO3-	1.89E-10
HSiO3-	1.05e-50
HSO4-	8.19E-15
K+	7.20E-02
Mg++	2.20E-09
Na+	7.00E-02
OH-	3.69E-03
SiO2(aq)	1.77E-07

Table B.11. Concentration Initial Condition: Concrete

Aqueous Species	mol/L
Al+++	5.09E-28
Ca++	2.53E-03
H2O	55.508
HCO3-	1.89E-10
HSiO3-	1.05e-50
HSO4-	8.19E-15
K+	7.20E-02
Mg++	2.20E-09
Na+	7.00E-02
OH-	3.69E-03
SiO2(aq)	1.77E-07

Table B.12. Concentration Initial Condition: Grout

Aqueous Species	mol/L
Al+++	1.08E-06
Ca++	6.60E-06
H2O	55.508
HSiO3-	2.52E-52
HSO4-	9.38E-20
HCO3-	2.82E-03
Mg++	6.13E-18
OH-	6.12E-04
K+	2.43E-08
Na+	1.56E-09
SiO2(aq)	5.50E-12
SO4--	2.61E-10
CaSO4(aq)	1.00E-01
CO3--	3.41E-02
CO2(aq)	4.30E-08

Table B.13. Concentration Initial Condition: Sand/Soil/Gravel

Aqueous Species	mol/L
Al+++	1.08E-06
Ca++	1.00E-05
H2O	55.508
HSiO3-	5.54E-09
HSO4-	1.97E-11
HCO3-	2.46E-08
K+	1.00e-06
Mg++	1.00e-06
OH-	9.96E-06
Na+	1.00e-06
SiO2(aq)	5.00E-06

References

Bacon DH and BP McGrail. 2005. *Waste Form Release Calculations for the 2005 Integrated Disposal Building Performance Assessment*. PNNL-15198, Pacific Northwest National Laboratory, Richland, Washington.

Savage D, D Noy, and M Mihara. 2002. "Modelling the interaction of bentonite with hyperalkaline fluids." *Applied Geochemistry,* 17:207–233.

Trotignon L, H Peycelon, and X Bourbon. 2006. "Comparison of performance of concrete barriers in a clayey geological medium." *Physics and Chemistry of the Earth,* 31:610–617.

Appendix C

CRUNCH Verification

Appendix C: CRUNCH Verification

As part of the quality assurance/quality control for software, a verification problem was run for the reactive transport simulator CRUNCH (Steefel 2001, Steefel and Yabusaki 1996). CRUNCH output was used to identify potential secondary mineral precipitates that served as input to the STOMP simulator.

CRUNCH output was compared with the EQ3/6, a software package used to perform geochemical modeling computations encompassing fluid mineral interactions and/or solution-mineral-equilibria in aqueous systems (Wolery and Jarek 2003, Wolery and Daveler 1992). The software package is composed of two major components: EQ3NR, a speciation-solubility code; EQ6, a reaction path modeling code to simulate water/rock interaction or fluid mixing in either a pure reaction progress mode or a time-dependent or kinetic mode. Like CRUNCH, the EQ3/6 software deals with the concepts of thermodynamic equilibrium, irreversible mass transfer, and reaction kinetics.

A simple seawater mixing problem that is part of a suite of sample EQ3/6 problems is used for comparison (swphcl.3i), modified to use the Davies equation for activity coefficients. Given an initial concentration of seawater, both codes performed aqueous speciation reactions and identified potential mineral precipitates. Results of the aqueous speciation appear in Table C.1 and demonstrate reasonable agreement. Table C.2 shows that CRUNCH identified a larger set of potential secondary minerals, but all of the minerals identified in the EQ3/6 simulation were also identified in the CRUNCH simulation.

Table C.1. Aqueous Speciation

Species Name	EQ3/6	CRUNCH
Ca++	9.20E-03	9.29E-03
CaCl+	2.19E-04	2.26E-04
CaCl2(aq)	6.12E-05	5.60E-05
CaCO3(aq)	3.16E-05	2.77E-05
CaHCO3+	3.03E-05	3.28E-05
CaOH+	7.07E-08	6.85E-08
CaSO4(aq)	7.43E-04	6.59E-04
Cl-	5.23E-01	5.25E-01
CO2(aq)	1.20E-05	1.35E-05
CO3--	3.19E-05	3.02E-05
H+	8.56E-09	8.81E-09
HCl(aq)	4.55E-10	1.17E-08
HCO3-	1.31E-03	1.29E-03
HSO4-	2.27E-09	2.25E-09
K+	9.92E-03	9.98E-03
KCl(aq)	7.89E-05	6.56E-05
KOH(aq)	3.94E-09	3.08E-09
KSO4-	2.09E-04	1.59E-04
Mg++	4.24E-02	4.07E-02
MgCl+	3.67E-03	4.61E-03
MgCO3(aq)	6.54E-05	6.98E-05
MgHCO3+	1.36E-04	1.80E-04
MgSO4(aq)	6.85E-03	7.58E-03
Na+	4.42E-01	4.45E-01
NaCl(aq)	1.83E-02	1.63E-02
NaCO3-	1.04E-05	8.33E-06
NaHCO3(aq)	3.92E-04	3.72E-04
NaOH(aq)	8.12E-08	6.73E-08
NaSO4-	8.10E-03	6.66E-03
OH-	2.44E-06	2.21E-06
SO4--	1.23E-02	1.32E-02

Table C.2. Potential Secondary Minerals

Mineral	CRUNCH	EQ3/6
Anhydrite	x	x
Antarcticite	x	
Aphthitalite	x	
Aragonite	x	x
Arcanite	x	x
Artinite	x	x
Bassanite	x	x
Bischofite	x	
Bloedite	x	x
Bogusite	x	
Brucite	x	x
Burkeite	x	
Ca2Cl2(OH)2.H2O	x	
Ca4Cl2(OH)6.13H2	x	
CaSO4.0.5H2O(bet	x	x
Calcite	x	x
Carnallite	x	
Chloromagnesite	x	
Dolomite	x	x
Dolomite-dis	x	x
Dolomite-ord	x	x
Epsomite	x	x
Gaylussite	x	x
Glauberite	x	x
Gypsum	x	x
Halite	x	x
HCl(c)	x	
Hexahydrite	x	x
Huntite	x	x
Hydromagnesite	x	x
Hydrophilite	x	
Ice	x	x
K2CO3.1.5H2O	x	
K2O	x	
K3H(SO4)2	x	
K8H4(CO3)6.3H2O	x	
KMgCl3	x	
KMgCl3.2H2O	x	
KNaCO3.6H2O	x	
Kainite	x	x
Kalicinite	x	x
Kieserite	x	x
Lansfordite	x	x
Leonite	x	
Lime	x	
Magnesite	x	x
Mercallite	x	
Mg1.25SO4(OH)0.5	x	x
Mg1.5SO4(OH)	x	x
MgCl2.2H2O	x	

Table C.2 (contd)

Mineral	CRUNCH	EQ3/6
MgCl2.4H2O	x	
MgCl2.H2O	x	
MgOHCl	x	
MgSO4	x	
Mirabilite	x	x
Misenite	x	
Monohydrocalcite	x	x
Na2CO3	x	x
Na2CO3.7H2O	x	x
Na2O	x	
Na3H(SO4)2	x	
Na4Ca(SO4)3.2H2O	x	x
Nahcolite	x	x
Natron	x	x
Nesquehonite	x	x
Oxychloride-Mg	x	x
Pentahydrite	x	x
Periclase	x	x
Picromerite	x	x
Pirssonite	x	x
Polyhalite	x	
Portlandite	x	
Starkeyite	x	x
Sylvite	x	x
Syngenite	x	x
Tachyhydrite	x	
Thenardite	x	x
Thermonatrite	x	x
Trona-K	x	

References

Steefel CI. 2001. *GIMRT: Software for modeling multicomponent, multidimensional reactive transport. Version 1.2. User's guide*. UCRL-MA-143182. Lawrence Livermore National Laboratory, Livermore, California.

Steefel CI and SB Yabusaki. 1996. *OS3D/GIMRT: Software for multicomponent–multidimensional reactive transport: User's manual and programmer's guide*. PNL-11166, Pacific Northwest National. Laboratory, Richland, Washington.

Wolery TJ and SA Daveler. 1992. *EQ6, A Computer program for Reaction Path Modeling of Aqueous Geochemical System: Theoretical Manual, User's Guide, and Related Documentation,* Version 7.0). Lawrence Livermore National Laboratory, Livermore, California.

Wolery TJ and RL Jarek. 2003. *Software User's Manual EQ3/6,* Version 8.0. 10813-UM-8.0-00, U.S. Department of Energy, Office of Civilian Radioactive Waste Management, Office of Repository Development, Las Vegas, Nevada.

Distribution

No. of
Copies

5 Fluor Hanford

R. Clinton	T5-49
E.R. Jacobs	S2-42
J.R. Robertson	H8-46
J.M. Steffen	R3-60
M. Stevens	R3-60

5 Pacific Northwest National Laboratory

Y. Chen	K9-36
V.L. Freedman (2)	K9-36
J.M. Keller	BPO
Z.F. Zhang	K9-36